Title
HOT Lane Simulation Tools

Authors
Horowitz, Roberto
Kurzhanskiy, Alex A.
Wright, Mathew

Publication Date
2018-06-25

HOT Lane Simulation Tools

Roberto Horowitz, Alex A. Kurzhanskiy, Mathew Wright

December 20, 2016

Contents

List of Figures

List of Tables

Acknowledgement

This research was sponsored by the Division of Research, Innovation and System Information (DRISI) of the California Department of Transportation. We especially thank Bradley Mizuno and Lai Saetern for their diligent project management and valuable guidance.

Chapter 1

Introduction

1.1 Overview

This report describes the simulation model and software for freeway corridors with High-Occupancy Vehicle (HOV) and High-Occupancy or Tolled (HOT) lanes, and the model calibration methodology. It is organized as follows.

- Chapter 2 covers the project methodology.
  - Section 2.1 sets up a context by a high-level description of the simulation framework.
  - Section 2.2 introduces the underlying traffic model.
  - Section 2.3 shows how the proposed traffic model accommodates different HOV lane configurations.
  - Section 2.4 explains how this model is extended to incorporate an HOT facility.
  - Section 2.5 describes the input data required by the simulation framework.
  - Section 2.6 describes the simulation output data performance measures computed from it, and the way they are reported.
  - Section 2.7 discusses how different model elements are put together and calibrated.

- Chapter 3 presents simulation case studies.
  - Section 3.1 presents the model of I-680 North freeway in Contra Costa County with full access HOV lane.
  - Section 3.2 presents the model of I-210 East freeway in Los Angeles County with limited access HOV lane.
  - Section 3.3 presents the model of the HOT controller calibrated based on the FasTrak transponder data on I-10 West in Los Angeles County and the simulation of I-10 West segment with an HOT gate and dynamic pricing.
- Chapter 4 concludes the report.

1.2 Problem

Inefficient traffic management and/or vehicle demand exceeding road network capacity are the most common causes of recurrent congestion [11]. High-occupancy-vehicle (HOV) lanes were proposed and adopted throughout the U.S. as an attempt at demand management: by allowing vehicles with multiple occupants exclusive access to a separate lane, civic authorities aimed to incentivize carpooling and reduce the number of cars on the road. HOV lanes can be "2+", admitting cars with two or more occupants, or "3+", which admit cars with at least three occupants. It is theorized that an HOV lane would have fewer cars and faster speed than the adjacent general-purpose (GP) lane, rewarding people traveling in carpools. In reality, however, this is not always the case. As it is evident from the case study of I-210 East in Los Angeles, presented in Section 3.2, the congestion patterns in both GP and HOV lanes are similar: HOV 2+ demand is so high that this HOV facility practically becomes another GP lane. One way to reduce the HOV demand in this case would be to convert the HOV 2+ lane into HOV 3+. A potential flaw of this approach, however, could be the underutilization of the HOV 3+ lane due to the exclusion of all two-person HOVs, and even larger congestion in the GP lane. Underutilization is what HOV lanes are being criticized for since their inception, with some saying they did not deliver on their promised demand reduction and did not substantially mitigate congestion in the GP lanes [9, 6]. This criticism led to the concept of high-

occupancy or tolled (HOT) lanes. Available to high-occupancy vehicles without charge, an HOT lane admits other vehicles if they pay a fee, which can be fixed or adjustable based on demand. The idea is that acceptance of more than just high-occupancy vehicles would lead to higher utilization of HOT lanes compared to their HOV counterparts. A dynamic pricing mechanism should control the HOT demand, making it possible to not let the speed in the HOT lane drop below 45 mph. Thus, the solution for I-210 managed lane could be to make it HOV 3+ or tolled facility. The proper operation of HOV/T lanes requires the combination of both, effective supply and demand management. There is a need for methods and tools that enable quick quantitative assessment of scenarios and operational strategies in terms of benefits they provide for freeway operation and revenue.

The research described in the current report builds upon the work conducted in 2006-14 in the Caltrans-sponsored UC Berkeley projects, Tools for Operational Planning (TOPL) [16] and Connected Corridors [2]. Our proposed HOV/T model is a modification of the Link-Node Cell Transmission Model [10] developed by TOPL. Our simulation framework [4] is constructed around the Berkeley Advanced Traffic Simulator (BeATS) [1] developed by Connected Corridors.

1.3 Objective

The aim of the current project was to develop a macroscopic freeway simulation model with an HOV/T lane, which could be calibrated based on measured vehicle counts and speeds and used for efficient evaluation of operational scenarios on freeways with HOV/T lanes.

Working toward this goal, we delivered:

1. the simulation model for HOV/T lanes implemented in BeATS;
2. calibration methodology for the proposed model;
3. analysis of pricing and traffic flow data from an HOT lane;
4. simulation framework for setting up operational scenarios and evaluating results;

5. case studies for HOV/T lanes with different configurations — full access HOV lane on I-680 North in Contra Costa County; limited access HOV lane on I-210 East in Los Angeles; and limited access HOT lane on I-10 West in Los Angeles.

1.4 Scope

Current list of HOT lane facilities in California is given in Table 1.1, spanning over 180 miles. HOT facilities are becoming popular in the U.S. For example, in the San Francisco Bay Area alone, the Metropolitan Transportation Commission (MTC) promises the implementation of a 550-mile express lane network by 2035, and all of it will be managed with dynamic pricing strategies.

Facility	Description
I-10	14 miles in each direction
I-15	20 miles in each direction
I-110	11 miles in each direction
I-580	14 miles in each direction
I-680 Milpitas - Sunol	14 miles South Bound
I-880 / SR-237	4 miles in each direction
SR-91	10 miles in each direction
I-680 San Ramon - Walnut Creek	12 miles in each direction expected to open in spring 2017

Table 1.1: List of HOT facilities in California.

Proper deployment and management of HOV/T facilities relies on the continuous process of:

1. obtaining and analyzing traffic measurement data;
2. operations planning — simulating various scenarios and operational strategies; and
3. implementing the most promising operational strategies in the field.

This process requires a fast and trusted traffic simulator for the rapid quantitative assessment of a large number of operational strategies for the road network under various scenarios. The research presented hereby is a necessary step toward achieving this goal.

Chapter 2

Methodology

2.1 Simulation Framework

The simulation framework that we developed in the course of the project is presented in Figure 2.1.

The centerpiece of the workflow is the Berkeley Advanced Traffic Simulator (BeATS), an open source macroscopic traffic simulation package written in Java. It takes an XML configuration file describing the structure of the road network, model parameters, controllers, incoming and outgoing flows, as input; runs the simulation; and generates output consisting of traffic densities, flows and speeds in the links of the road network evolving in time. This simulation output can then be used to compute performance measures, such as:

- Vehicle Miles Traveled (VMT);
- Vehicle Hours Traveled (VHT);
- Delay in vehicle-hours computed for the portion of traffic traveling below free flow speed;
- On-ramp queues.

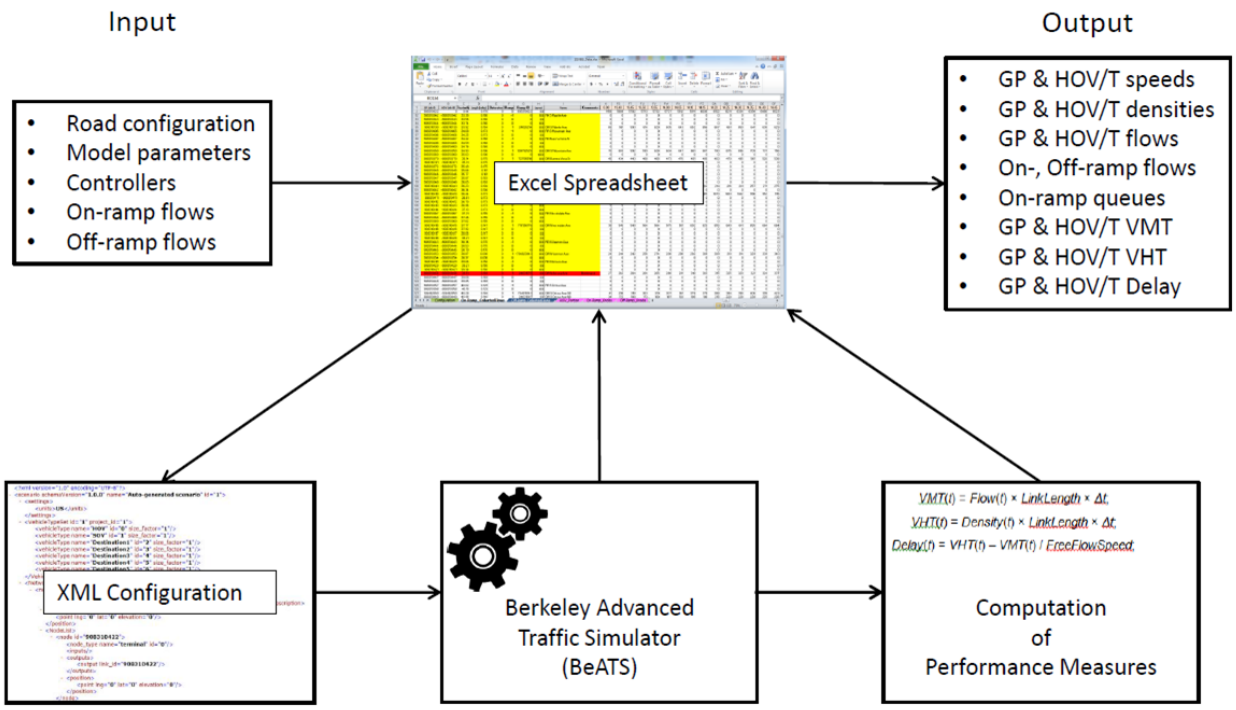

Figure 2.1: Simulation framework — workflow diagram.

The user interacts with the simulation model through the Excel spreadsheet that is used to enter all the necessary input data and then, after the simulation, inspect the simulation results, which are recorded there. The connections between the spreadsheet and BeATS, that is: generation of the XML configuration file from spreadsheet; simulation start and stop; computation of performance measures; and sending the simulation results back to the spreadsheet is taken care of by the toolbox [4] that is presently implemented in MATLAB.

Next, we shall describe how the traffic model of BeATS works.

2.2 Traffic Model

We model traffic flow in a road network consisting of links $\mathcal{L}$ and nodes $\mathcal{N}$, where links represent stretches of roads, and nodes represent junctions that connect links. A node always has at least one input and at least one output link. A link is called *ordinary* if it has both begin and end nodes. A link with no begin node is called *origin*, and a link with no end node is called *destination*. Origins

are links through which vehicles enter the system, and destinations are links that let vehicles out. The traffic state at each moment of time is defined by the number of vehicles of different classes in every link. Different vehicle classes are needed to distinguish between low-occupancy vehicles (LOVs) and high-occupancy vehicles (HOVs). For HOT lanes the additional class is needed — LOVs ready to pay.

To describe the model, we will use the following notation:

- l — identifier of a link in the road network.
- ν — identifier of a node in the road network.
- C — number of traffic classes (LOV, HOV, etc.).
- c — index of a traffic class ($c = 1, \ldots, C$).
- v_l^f — free flow speed in link l.
- w_l^f — congestion wave speed in link l.
- n_l^J — maximum number of vehicles in link l, also referred to as *jam density*.
- F_l — capacity of link l.
- $n_l^- = \frac{w_l n_l^J}{v_l^f + w_l}$ and $n_l^+ = \frac{F_l}{v_l^f}$ — low and high critical densities of link l.
- $n_l^c(t)$ — number of vehicles of class c in link l at time t.
- $n_l(t) = \sum_{c=1}^{C} n_l^c(t)$ — total number of vehicles in link l at time t.
- $f_l^{c,in}(t)$ — flow of class c entering link l at time t.
- $f_l^{c,out}(t)$ — flow of class c leaving link l at time t.
- M_ν — number of input links of node ν.
- N_ν — number of output links of node ν.
- i — index of an input link ($i = 1, \ldots, M_\nu$) of node ν.

- j — index of an output link ($j = 1, \ldots, N_\nu$) of node ν.
- $p_{\nu,i}$ — input link priority at node ν.
- $\beta^c_{\nu,ij} \in [0,1]$ — split ratios that distribute traffic of a given commodity c coming from input link i between output links at node ν, $\sum_{j=1}^{N} \beta^c_{\nu,ij} = 1$.
- $\boldsymbol{\eta}^i_{\nu,j'j} = [y,z] \subseteq [0,1]$ — mutual restriction intervals that should be interpreted as follows:
  - $\boldsymbol{\eta}_{\nu,j'j} = [0,1]$ — congestion in the output link j' of node ν affects flow directed from the input link i to the output link j in full. Obviously, $\boldsymbol{\eta}^i_{\nu,jj} \equiv [0,1]$ for all i.
  - $\boldsymbol{\eta}^i_{\nu,j'j} = [0,0]$ (or any other interval of zero length) — traffic state in the output link j' does not influence the flow from the input link i to the output link j at node ν.
  - $\boldsymbol{\eta}^i_{\nu,j'j} = [y,z] \subset [0,1]$ — traffic state in the output link j' affects a $|\boldsymbol{\eta}^i_{\nu,j'j}| = z - y$ portion of the flow directed from the input link i to the output link j of node ν. We specify this influence as an interval, not just a scalar, to capture the summary effect of multiple output links that may restrict flow to the output link j.
- $f^c_{\nu,ij}(t)$ — flow of class c directed from input link i to the output link j of node ν at time t.

Detailed explanation of the meaning of all these terms can be found in [17].

Each link $l \in \mathcal{L}$ is characterized by its length and the fundamental diagram, a flow-density relationship presented in Figure 2.2. A fundamental diagram is defined by four values: capacity F_l, free flow speed v^f_l, congestion wave speed w_l and the jam density n^J_l.[1]

In this report we assume that densities, flows and speeds are *normalized* by link lengths and the simulation time step; [2] and that free flow speed v^f_l and congestion wave speed w_l satisfy the Courant-Friedrichs-Lewy (CFL) condition [7]: $0 \le v^f_l, w_l \le 1$. [3] The values $n^-_l = \frac{w_l n^J_l}{v^f_l + w_l}$ and $n^+_l = \frac{F_l}{v^f_l}$ are called *low* and *high critical density* respectively. Unless $n^-_l = n^+_l$, when it assumes triangular shape,

[1] For the sake of notation, in this report we assume these values to be fixed, but in general the may be time-varyinng.

[2] Given original (not normalized) capacity $\tilde{F}_l$ specified in vehicles per hour (vph), free flow speed $\tilde{v}^f_l$ and congestion wave speed $\tilde{w}_l$ specified in miles per hour (mph), and jam density $\tilde{n}^J_l$ specified in vehicles per mile (vpm), as well as link length Δx_l and simulation time step Δt, normalized values are $F_l = \tilde{F}_l \Delta t$ specified in vehicles per time period Δt, $v^f_l = \tilde{v}^f_l \frac{\Delta t}{\Delta x_l}$ and $w_l = \tilde{w}_l \frac{\Delta t}{\Delta x_l}$, both unitless, and $n^J_l = \tilde{n}^J_l \Delta x_l$ specified in vehicles.

[3] The CFL condition is the necessary condition for convergence while solving hyperbolic PDEs numerically.

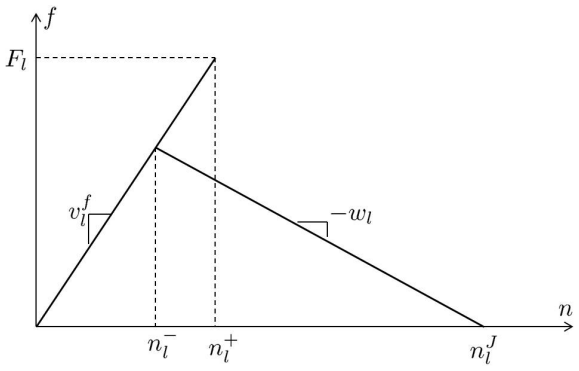

Figure 2.2: Fundamental diagram.

the fundamental diagram is not a function of density: $n_l(t) \in \left(n_l^-, n_l^+\right]$ admits two possible flow values.

Each node $\nu \in \mathcal{N}$ with M_ν input and N_ν output links is characterized by time dependent mutual restriction intervals $\{\boldsymbol{\eta}_{jj'}^i(t)\}$, input link priorities $\{p_i(t)\}$ and partially defined split ratios $\{\beta_{ij}^c(t)\}$, [4] where C is the number of vehicle types; $i = 1, \ldots, M_\nu$, $j, j' = 1, \ldots, N_\nu$ and $c = 1, \ldots, C$.

The state of the system at time t is described by the number of vehicles per traffic class in each link: $\vec{n}_l(t) = \left[n_l^1(t), \ldots, n_l^C(t)\right]^T$, where $n_l^c(t)$ represents the number of vehicles of type c in link l at time t. In our notation, $n_l(t) = \sum_{c=1}^C n_l^c(t)$. The state update equation for link $l \in \mathcal{L}$ is:

$$\vec{n}_l(t+1) = \vec{n}_l(t) + \left(\vec{f}_l^{in}(t) - \vec{f}_l^{out}(t)\right), \tag{2.2.1}$$

where $\vec{f}_l^{in}(t) = \left[f_l^{1,in}(t), \ldots, f_l^{C,in}(t)\right]^T$ is the vector of commodity flows coming into link l during this time step, and $\vec{f}_l^{out}(t) = \left[f_l^{1,out}(t), \ldots, f_l^{C,out}(t)\right]^T$ is the vector of commodity flows leaving link l during this time step.

For ordinary and destination links, $\vec{f}_l^{in}(t)$ is obtained from the begin node: given a begin node ν with M_ν input links,

$$f_l^{c,in}(t) = \sum_{i=1}^{M_\nu} f_{il}^c(t), \quad c = 1, \ldots, C. \tag{2.2.2}$$

[4] Split ratios may also be fully defined or fully undefined.

For origin links,

$$f_l^{c,in}(t) = d_l^c(t), \tag{2.2.3}$$

where $d_l^c(t)$ denotes demand of class c at time t, which is an exogenous input to the model, specified in vehicles per simulation step Δt.

For ordinary and origin links, $\vec{f}_l^{out}(t)$ is obtained from the end node: given an end node ν with N_ν output links,

$$f_l^{c,out}(t) = \sum_{j=1}^{N_\nu} f_{lj}^c(t), \quad c = 1, \ldots, C. \tag{2.2.4}$$

For destination links,

$$f_l^{c,out}(t) = v_l^f n_l^c(t) \min\left\{1, \frac{F_l}{\sum_{c'=1}^{C} v_l^f n_l^{c'}(t)}\right\}, \quad c = 1, \ldots, C. \tag{2.2.5}$$

For each link $l \in \mathcal{L}$ we will also define a congestion metastate:

$$\theta_l(t) = \begin{cases} 0 & n_l(t) \le n_l^-, \\ 1 & n_l(t) > n_l^+, \\ \theta_l(t-1) & n_l^- < n_l(t) \le n_l^+. \end{cases} \tag{2.2.6}$$

This metastate helps determining which constraint of the fundamental diagram is activated when we compute the receive function for a link.

Now we can formally describe the simulation model that runs for T time steps.

1. Initialize:

$$\begin{aligned} n_l^c(0) &:= n_{l,0}^c; \\ \theta_l(0) &:= \theta_{l,0}; \\ t &:= 0 \end{aligned}$$

for all $l \in \mathcal{L}$ and $c = 1, \ldots, C$, where $n^c_{l,0}$ and $\theta_{l,0}$ are the initial conditions.

2. Apply all the control functions that modify system parameters (fundamental diagrams, input priorities) and/or system state. A control function may represent ramp metering, variable speed limit, managed lane policy, etc. Control functions may be *open-loop* (if they depend only on time) and *closed-loop* (if they depend on time and system state). This step is optional.

3. For each link $l \in \mathcal{L}$ and commodity $c = 1, \ldots, C$ define the *send* function (demand):

$$S^c_l(t) = \begin{cases} v^f_l n^c_l(t) \min\left\{1, \frac{F_l}{v^f_l \sum_{c=1}^C n^c_l(t)}\right\}, & l \text{ is an ordinary link or a destination,} \\ d^c_l(t) \min\left\{1, \frac{F_l}{\sum_{c=1}^C d^c_l(t)}\right\}, & l \text{ is an origin.} \end{cases} \tag{2.2.7}$$

4. For each link $l \in \mathcal{L}$ define the *receive* function (supply):

$$R_l(t) = \begin{cases} (1 - \theta_l(t))\, F_l + \theta_l(t) w_l \left(n^J_l - \sum_{c=1}^C n^c_l(t)\right), & l \text{ is an ordinary link or a destination,} \\ \infty, & l \text{ is an origin.} \end{cases} \tag{2.2.8}$$

5. For each node $\nu \in \mathcal{N}$ with input links $i = 1, \ldots, M_\nu$, and output links $j = 1, \ldots, N_\nu$, that has undefined split ratios,[5] given its input link priorities $\{p_i(t)\}$, send functions $S^c_i(t)$ and receive functions $R_j(t)$, compute the undefined split ratios $\{\beta^c_{\nu,ij}(t)\}$ with the objective:

$$\min\left\{\max_j \max_i \left(\frac{\sum_{c=1}^C \beta^c_{\nu,ij} S^c_i}{p_{ij} R_j} \sum_{i=1}^{M_\nu} p_{ij}\right) - \min_j \min_i \left(\frac{\sum_{c=1}^C \beta^c_{\nu,ij} S^c_i}{p_{ij} R_j} \sum_{i=1}^{M_\nu} p_{ij}\right)\right\}, \tag{2.2.9}$$

where:

- the optimization problem is solved at every time step t, and argument (t) is implied, but omitted to make the notation easier;
- $p_{ij} = \frac{\sum_{c=1}^C \beta^c_{\nu,ij} S^c_{ij}}{\sum_{c=1}^C S^c_i} p_{\nu,i}$.

The algorithm for solving this optimization problem is described in [17].

[5] Not all split ratios may be difined a priori: e.g. HOVs may decided between the HOV and the GP lanes based on the current traffic condition, but not ahead of time.

6. For each node $\nu \in \mathcal{N}$ with input links $i = 1, \ldots, M_\nu$, and output links $j = 1, \ldots, N_\nu$, given its mutual restriction intervals $\{\boldsymbol{\eta}^i_{\nu,jj'}(t)\}$, input link priorities $\{p_{\nu,i}(t)\}$ and split ratios $\{\beta^c_{\nu,ij}(t)\}$, send functions $S^c_i(t)$ and receive functions $R_j(t)$, compute input-output flows $f^c_{\nu,ij}(t)$ by solving the following optimization problem:

$$\max \left(\sum_{i=1}^{M} \sum_{j=1}^{N} \sum_{c=1}^{C} f^c_{ij} \right), \tag{2.2.10}$$

subject to:

$$f^c_{ij} \geq 0, \;\; i = 1, \ldots, M, \; j = 1, \ldots, N, \; c = 1, \ldots, C \;\; \text{— non-negativity constraint;} \tag{2.2.11}$$

$$f^c_{ij} \leq S^c_{ij}, \;\; i = 1, \ldots, M, \; j = 1, \ldots, N, \; c = 1, \ldots, C \;\; \text{— demand constraint;} \tag{2.2.12}$$

$$\sum_{i=1}^{M} f_{ij} \leq R_j, \;\; j = 1, \ldots, N \;\; \text{— supply constraint;} \tag{2.2.13}$$

$$\frac{f^c_{ij}}{f_{ij}} = \frac{S^c_{ij}}{S_{ij}}, \;\; i = 1, \ldots, M, \; j = 1, \ldots, N, c = 1, \ldots, C \;\; \text{— proportionality constraint for commodity flows;} \tag{2.2.14}$$

$$\left.\begin{array}{ll} \text{(a)} & \text{For each input link } i, \text{ such that} \\ & \sum_{j=1}^{N} f_{ij} < S_i, \;\; W_i \neq \emptyset; \\ \text{(b)} & \text{For each input link } i, \text{ such that } W_i \neq \emptyset, \\ & f_{ij} \geq \frac{p_{ij}}{\sum_{i'=1}^{M} p_{i'j}} R_j, \;\; \forall j \in W_i. \end{array}\right\} \;\; \text{— priority constraint;} \tag{2.2.15}$$

$$f_{ij} \leq S_{ij} - \mathcal{A} \left(\bigcup_{j' \in W_i \setminus \{j\}} \mathcal{Q}^i_{j'j} \right), \;\; i = 1, \ldots, M, \; j = 1, \ldots, N \;\; \text{— relaxed first-in-first-out constraint;} \tag{2.2.16}$$

where:

- in all the terms, the subindex ν is implied, but omitted to make the notation easier;
- the optimization problem is solved at every time step t, and argument (t) is implied, but omitted to make the notation easier;
- $S^c_{ij} = \beta^c_{ij} S^c_i$;

- $S_{ij} = \sum_{c=1}^{C} S_{ij}^c$;
- $f_{ij} = \sum_{c=1}^{C} f_{ij}^c$;
- $p_{ij} = \frac{\sum_{c=1}^{C} S_{ij}^c}{\sum_{c=1}^{C} S_i^c} p_i$;
- $W_i = \left\{ j^* : \ \ S_{ij^*} > 0; \ \ p_{i'j^*} f_{ij^*} \geq p_{ij^*} f_{i'j^*}, \ \ \forall i' \neq i \right\}$;
- $\mathcal{Q}_{j'j}^i = \boldsymbol{\eta}_{j'j} \times \left[\frac{f_{ij'}}{S_{ij'}} S_{ij}, S_{ij} \right]$, with '$\times$' denoting a Cartesian product; and
- $\mathcal{A}(\cdot)$ denotes the area of a two-dimensional shape.

The algorithm for solving this optimization problem is described in [17].

7. For each link $l \in \mathcal{L}$, compute $\vec{f}_l^{in}(t)$ using expressions (2.2.2)-(2.2.3) and $\vec{f}_l^{out}(t)$ using expressions (2.2.4)-(2.2.5).

8. For each link $l \in \mathcal{L}$, update the state $\vec{n}_l(t+1)$ according to the conservation equation (2.2.1), and the metastate $\theta_l(t+1)$ according to its definition (2.2.6).

9. If $t = T$, then stop, otherwise set $t := t + 1$ and return to step 2.

Traffic speed for link l is computed as a ratio of total flow leaving this link to the total number of vehicles in this link:

$$v_l(t) = \begin{cases} \frac{\sum_{c=1}^{C} f_l^{c,out}(t)}{\sum_{c=1}^{C} n_l^c(t)}, & \text{if } \sum_{c=1}^{C} n_l^c(t) > 0, \\ v_l^f, & \text{otherwise.} \end{cases} \tag{2.2.17}$$

Defined this way, $v_l(t) \in [0, v_l^f]$.

Next, we shall describe how HOV facilities are implemented within this traffic model.

2.3 HOV Model

We will consider two types of HOV configurations: *full access* and *separated with limited access*. Full access is the configuration where the HOV lane is just another freeway lane, to (from) which eligible vehicles may switch from (to) the general purpose (GP) lane anywhere. Typically, a full

access lane is designated an HOV lane only during certain periods of the day, and at other times it serves as a GP lane. On the other hand, a separated HOV lane allows traffic from and to the GP lane only at certain locations, called *gates*, and it admits only HOV traffic at all times. The implemented HOV access scheme depends on jurisdiction; for example, full access lanes are common in Northern California, and separated HOV lanes are common in Southern California. Modeling of these two configurations is described next.

2.3.1 Full Access HOV Lane

A full access HOV lane configuration is presented in Figure 2.3: GP and HOV links are parallel with the same geometry and share the same begin and end node pairs; traffic flow exchange between GP and HOV lanes can happen at every node. Links that are too long may be broken up into smaller ones by creating more nodes, such as nodes 2 and 3 in Figure 2.3. Generally, fundamental diagrams for parallel GP and HOV links are different.

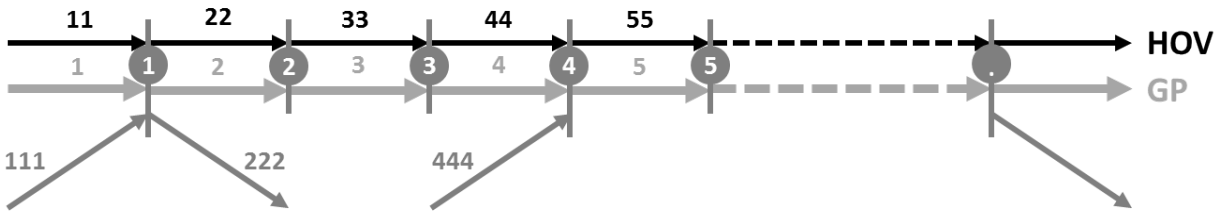

Figure 2.3: Freeway with full access HOV lane.

We introduce two traffic commodities ($C = 2$): $c = 1$ corresponds to the low occupancy vehicle (LOV) traffic, and $c = 2$ corresponds to the HOV traffic. When HOV lane is active, $c = 1$-traffic is confined to the GP lane, whereas $c = 2$-traffic can use both GP and HOV lanes. E.g., for node 1 in

Figure 2.3 this policy translates to:

$$
\begin{array}{llll}
\beta^1_{1,2} = 1 - \beta^1_{1,222} & \beta^1_{1,22} = 0 & \beta^1_{1,222}; & \\
\beta^1_{11,2} = 1 - \beta^1_{11,222} & \beta^1_{11,22} = 0 & \beta^1_{11,222}; & \\
\beta^1_{111,2} = 1 - \beta^1_{111,222} & \beta^1_{111,22} = 0 & \beta^1_{111,222}; & \\
\beta^2_{1,2} = \ ? & \beta^2_{1,22} = \ ? & \beta^2_{1,222} & \overline{\beta}^2_1 = 1 - \beta^2_{1,222}; \\
\beta^2_{11,2} = \ ? & \beta^2_{11,22} = \ ? & \beta^2_{11,222} & \overline{\beta}^2_{11} = 1 - \beta^2_{11,222}; \\
\beta^2_{111,2} = \ ? & \beta^2_{111,22} = \ ? & \beta^2_{111,222} & \overline{\beta}^2_{111} = 1 - \beta^2_{111,222},
\end{array}
\tag{2.3.1}
$$

where $\beta^c_{i,222}$, are given (for example, computed from off-ramp detector measurements), and β^2_{ij} are to be determined using the split ratio assignment from step 5 of the simulation algorithm, $i = 1, 11, 111$, $j = 2, 22$. Similarly, for node 2:

$$
\begin{array}{llll}
\beta^1_{2,3} = 1 & \beta^1_{2,33} = 0; & & \\
\beta^1_{22,3} = 1 & \beta^1_{22,33} = 0; & & \\
\beta^2_{2,3} = \ ? & \beta^2_{2,33} = \ ? & \overline{\beta}^2_2 = 1; & \\
\beta^2_{22,3} = \ ? & \beta^2_{22,33} = \ ? & \overline{\beta}^2_{22} = 1. &
\end{array}
\tag{2.3.2}
$$

When the HOV lane is deactivated and becomes available for LOV traffic, split ratios for GP and HOV output links are to be determined for both vehicle types. So, for node 1 we have:

$$
\begin{array}{lll}
\beta^c_{i,j} = \ ? & \beta^c_{i,222} & \overline{\beta}^c_i = 1 - \beta^c_{i,222}; \\
i = 1, 11, 111; \quad j = 2, 22; & c = 1, 2; &
\end{array}
\tag{2.3.3}
$$

and for node 2:

$$
\begin{array}{ll}
\beta^c_{i,j} = \ ? & \overline{\beta}^c_i = 1; \\
i = 2, 22; \quad j = 3, 33; & c = 1, 2.
\end{array}
\tag{2.3.4}
$$

In this report we do not insist on any particular way of setting link priorities. One common-sense approach inspired by Tampére et al. [15] would be to make priorities proportional to link capacities,

which for node 1 in Figure 2.3, will produce:

$$p_i = \frac{F_i}{F_1 + F_{11} + F_{111}}, \quad i = 1, 11, 111.$$

In some cases it makes sense to assign higher priorities to on-ramps. For example, if link 5 in Figure 2.3 has an auxiliary lane starting from node 4, which allows all (or almost all) traffic to enter freeway from on-ramp 444 even when link 5 is congested. In this situation we would set priority p_{444} proportional to $2F_{444}$. Thus, it is reasonable to set priorities of GP and HOV links proportional to their capacities, whereas on-ramp priorities depend on the configuration of the on-ramp and the freeway merging section.

Other parameters that largely depend on the freeway configuration are the mutual restriction intervals. Denote the number of sublanes[6] in links 1, 2 and 22 of Figure 2.3 L_1, L_2 and L_{22} respectively, and let $L_{1,222} < L_1$ be the number of sublanes in link 1, from which traffic can exit to the off-ramp 222. Then, one possible way of setting mutual restriction intervals would be:

$$\begin{array}{lll} \boldsymbol{\eta}^i_{2,2} = [0,1] & \boldsymbol{\eta}^i_{2,22} = \left[1 - \frac{1}{L_{22}}, 1\right] & \boldsymbol{\eta}^i_{2,222} = [0,1]; \\ \boldsymbol{\eta}^i_{22,2} = \left[0, \frac{1}{L_2}\right] & \boldsymbol{\eta}^i_{22,22} = [0,1] & \boldsymbol{\eta}^i_{22,222} = [0,0]; \\ \boldsymbol{\eta}^i_{222,2} = \left[1 - \frac{L_{1,222}}{L_1}, 1\right] & \boldsymbol{\eta}^i_{222,22} = [0,0] & \boldsymbol{\eta}^i_{222,222} = [0,1], \end{array} \tag{2.3.5}$$

for all input links of node 1: $i = 1, 11, 111$. With such mutual restriction intervals we suggest that shortage of supply in GP link 2 affects the whole flow to the off-ramp 222 ($\boldsymbol{\eta}^i_{2,222} = [0,1]$) and affects flow in one of the lanes of HOV link 22 ($\boldsymbol{\eta}^i_{2,22} = \left[1 - \frac{1}{L_{22}}, 1\right]$; shortage of supply in HOV link 22 affects flow in one of the lanes of GP link 2 ($\boldsymbol{\eta}^i_{22,2} = \left[0, \frac{1}{L_2}\right]$) and does not affect the off-ramp flow ($\boldsymbol{\eta}^i_{22,222} = [0,0]$); shortage of supply in the off-ramp 222 affects flow in GP link 2 proportionally to the ratio of the number of lanes that send traffic to the off-ramp in link 1 to the total number of lanes in that link ($\boldsymbol{\eta}^i_{222,2} = \left[1 - \frac{L_{1,222}}{L_1}, 1\right]$) and does not affect the flow in HOV link 22 ($\boldsymbol{\eta}^i_{222,22} = [0,0]$). A conservative alternative to this approach would be to set all mutual restriction intervals to 1.

The case study with the full access HOV lane is presented in Section 3.1.

[6] We use the term "sublane" here to avoid confusion with the term "lane", which throughout this report is synonymous to "facility". So, when we say that an HOV lane has 2 sublanes and a GP lane has 4 sublanes, we actually mean that the freeway has 2 HOV and 4 GP lanes.

2.3.2 Separated HOV Lane with Limited Access

The configuration of the separated HOV lane with limited access is presented in Figure 2.4: GP and HOV lanes are treated as two separate freeways that have some common nodes that allow flow exchange between these two freeways. These nodes are *gates*. In the freeway with a full access HOV lane discussed previously, every node is a gate. We can disable flow exchange at a given node by fixing split ratios so that they keep traffic in its lane. For example, to disable the gate (the flow exchange between the two lanes) at node 2 in Figure 2.3, we set $\beta^c_{2,3} = 1$ and $\beta^c_{22,33} = 1$ ($\beta^c_{2,33} = 0$ and $\beta^c_{22,3} = 0$), $c = 1, 2$. Thus, the full access HOV lane can be easily converted into the separated HOV lane by fixing split ratios everywhere but designated gate-nodes. In practice, a gate is stretch of freeway about 0.5 miles long, and, potentially, we can designate two or three nodes in a row as gates. However, we assume that a gate is a single node.

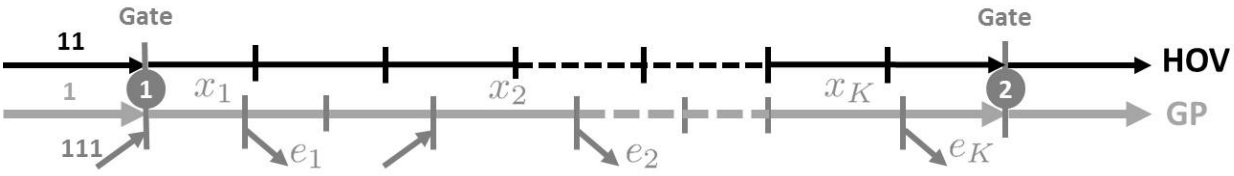

Figure 2.4: Freeway with separated HOV lane and gates.

For the separated HOV configuration, we suggest setting mutual restriction coefficients just as in the case of full access HOV lane, according to formula (2.3.5).

Directing Traffic from the HOV Lane to Off-Ramps

In the full access HOV model, we could direct traffic from the HOV lane to off-ramps by setting corresponding split ratios, e.g. $\beta^c_{11,222}$, $c = 1, 2$, for node 1 in configuration from Figure 2.3. The challenge of the separated HOV lane modeling is that generally gates do not coincide with off-ramp locations. Typically, there are between 2 and 5 off-ramps in the freeway segment from one gate to the next. Off-ramps in the GP road segment connecting two gates in Figure 2.4 are identified as exits $e_1, e_2, \ldots, e_K$, and they cannot be accessed directly from the HOV lane. Vehicles traveling in the HOV lane that intend to take one of the exits $e_1, \ldots, e_K$, must switch from the HOV lane to the GP lane at gate-node 1 and then be directed to the correct off-ramp.

To resolve this challenge, we introduce new traffic commodities in addition to already existing $c = 1$ (LOVs) and $c = 2$ (HOVs) that were introduced in the full access HOV lane model, Section 2.3.1. These additional commodities will be used to distinguish traffic by its destination off-ramp. Assuming that K is the largest number of off-ramps in the GP lane between two adjacent gates, altogether we have $C = K + 2$ traffic commodities: $c = 1, 2, e_1, \ldots, e_K$, where e_k indicates the destination off-ramp in reference to Figure 2.4. By definition, traffic of type $c = e_k$ *may exist* in the GP lane segment between gate 1 and off-ramp e_k, but there is *no traffic of this type* either in the GP lane segment between off-ramp e_k and gate 2 or in the HOV lane. To ensure this, we set *constant* split ratios:

$$\begin{aligned}
&\beta^{e_k}_{i,x_1} = 1, \quad i = 1, 11, 111, && \text{direct all } e_k\text{-type traffic to the GP lane at gate 1;} \\
&\beta^{e_k}_{x_k,e_k} = 1, && \text{direct all } e_k\text{-type traffic to off-ramp } e_k; \\
&\beta^{e_k}_{x_{k'},e_{k'}} = 0, \quad k' \neq k, && \text{do not send any } e_k\text{-type traffic to other off-ramps,}
\end{aligned} \tag{2.3.6}$$

where $k = 1, \ldots, K$, and x_k denotes the input GP link for the node that has the output link e_k (see Figure 2.4).

Now we explain how e_k-type traffic appears in the system. The original demand $d^c_l(\cdot)$ is specified at origin links l for commodities $c = 1, 2$, and $d^{e_k}_l(\cdot) \equiv 0$, $k = 1, \ldots, K$. Destination specific traffic appears in the HOV links that end at gate-nodes by assigning destinations to portions of the type-1 (LOV) and type-2 (HOV) traffic in those links. We propose incorporating this destination assignment into the step 2 of the simulation algorithm, applying control (Section 2.2) and using off-ramp split ratios $\beta^c_{x_k,e_k}$, $c = 1, 2$, $k = 1, \ldots, K$, to determine portions of HOV lane traffic to be assigned particular destinations. The destination assignment algorithm at a given time t, for a given HOV link ending with a gate-node, is described next. Without the loss of generality, we will refer to Figure 2.4 and the HOV link 11 ending at the gate-node 1 in this description.

1. Given are vehicle counts per commodity n^c_{11}, $c = 1, 2, e_1, \ldots, e_K$; free flow speed v_{11}; and off-ramp split ratios $\beta^1_{x_k,e_k}$ and $\beta^2_{x_k,e_k}$, $k = 1, \ldots, K$.[7]

[7] If a given GP segment connecting two adjacent gates has K' off-ramps, where $K' < K$, then assume $\beta^1_{x_k,e_k} = \beta^2_{x_k,e_k} = 0$ for $k \in (K', K]$.

2. Initialize:

$$\begin{aligned} \tilde{n}_{11}^{c}(0) &:= n_{11}^{c}, \quad c = 1, 2, e_1, \dots e_K; \\ k &:= 1. \end{aligned}$$

3. Assign e_k-type traffic:

$$\tilde{n}_{11}^{e_k}(k) = \tilde{n}_{11}^{e_k}(k-1) + \beta_{x_k,e_k}^{1} v_{11} \tilde{n}_{11}^{1}(k-1) + \beta_{x_k,e_k}^{2} v_{11} \tilde{n}_{11}^{2}(k-1); \tag{2.3.7}$$

$$\tilde{n}_{11}^{1}(k) = \tilde{n}_{11}^{1}(k-1) - \beta_{x_k,e_k}^{1} v_{11} \tilde{n}_{11}^{1}(k-1); \tag{2.3.8}$$

$$\tilde{n}_{11}^{2}(k) = \tilde{n}_{11}^{2}(k-1) - \beta_{x_k,e_k}^{2} v_{11} \tilde{n}_{11}^{2}(k-1). \tag{2.3.9}$$

4. If $k < K$, then set $k := k + 1$ and return to step 3.

5. Update the state:

$$n_{11}^{c} = \tilde{n}_{11}^{c}(K), \quad c = 1, 2, e_1, \dots, e_K.$$

The case study with the separated HOV lane is presented in Section 3.2.

The model of HOT facility builds on that of the HOV facility, and we shall describe it next.

2.4 HOT Model

To extend the proposed full access and gated HOV lane models to HOT, we introduce new vehicle class — *LOVs that are ready to pay* — following the notation of Section 2.3.1, $c = 3$. Just as $c = 2$-traffic, $c = 3$-traffic can use both GP and HOT lanes. E.g., for node 1 in Figure 2.5 this

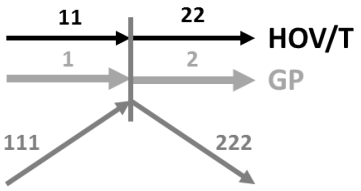

Figure 2.5: A node with 3 input and 3 output links representing a decision point.

policy translates to:

$$
\begin{array}{llll}
\beta^1_{1,2} = 1 - \beta^1_{1,222} & \beta^1_{1,22} = 0 & \beta^1_{1,222}; & \\
\beta^1_{11,2} = 1 - \beta^1_{11,222} & \beta^1_{11,22} = 0 & \beta^1_{11,222}; & \\
\beta^1_{111,2} = 1 - \beta^1_{111,222} & \beta^1_{111,22} = 0 & \beta^1_{111,222}; & \\
\beta^2_{1,2} = \ ? & \beta^2_{1,22} = \ ? & \beta^2_{1,222} & \overline{\beta}^2_1 = 1 - \beta^2_{1,222}; \\
\beta^2_{11,2} = \ ? & \beta^2_{11,22} = \ ? & \beta^2_{11,222} & \overline{\beta}^2_{11} = 1 - \beta^2_{11,222}; \\
\beta^2_{111,2} = \ ? & \beta^2_{111,22} = \ ? & \beta^2_{111,222} & \overline{\beta}^2_{111} = 1 - \beta^2_{111,222}, \\
\beta^3_{1,2} = \ ? & \beta^3_{1,22} = \ ? & \beta^3_{1,222} & \overline{\beta}^3_1 = 1 - \beta^3_{1,222}; \\
\beta^3_{11,2} = \ ? & \beta^3_{11,22} = \ ? & \beta^3_{11,222} & \overline{\beta}^3_{11} = 1 - \beta^3_{11,222}; \\
\beta^3_{111,2} = \ ? & \beta^3_{111,22} = \ ? & \beta^3_{111,222} & \overline{\beta}^3_{111} = 1 - \beta^3_{111,222},
\end{array}
\tag{2.4.1}
$$

where $\beta^c_{i,222}$, are given (for example, computed from off-ramp detector measurements), and β^c_{ij} are to be determined using the split ratio assignment from step 5 of the simulation algorithm (Section 2.2), $i = 1, 11, 111$, $j = 2, 22$, $c = 2, 3$. Thus, we will deal with $C = 3$, in the case of full access HOT lane, and with $C = K + 3$, in the case of gated HOT lane, traffic commodities.

The other component of the HOT model is the HOT controller consisting of two parts:

1. Calculation of the toll based on the vehicle flow in the HOT lane; and
2. Calculation of the portion of LOVs ready to pay given toll and reassigning vehicles between classes $c = 1$ and $c = 3$ accordingly.

Toll $\pi(\cdot)$ varies between its minimal and maximal values, $\pi_{\min}$ and $\pi_{\max}$, and is computed from the *flow-price curve*, depicted in Figure 2.6, where f^{in}_{22} denotes total flow entering link 22 in Figure 2.5. The flow-price curve is defined by the HOT lane operator in the form of lookup table.

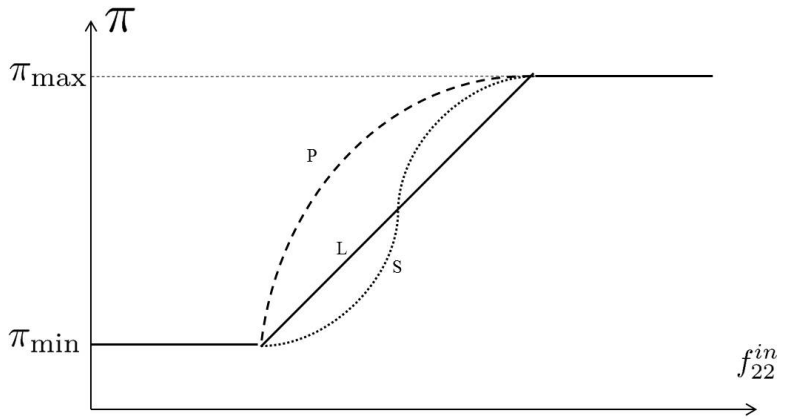

Figure 2.6: Flow-price curve: toll depends on the total flow entering the HOT link (link 22, as in Figure 2.5). Shown are linear (L), polynomial (P) and sigmoid (S) dependencies.

In the second part of the HOT controller we should determine the portion of LOVs ready to pay given price for using HOT lane. The readiess to pay may depend on multiple factors, most obvious of which are:

1. Toll value;
2. Difference in traffic density between GP and HOT lanes;
3. The estimated gain in travel time of the HOT lane over the GP lane; and
4. Travel time reliability.

In this project, we coonsidered readiness to pay depending on items 1 and 2 — toll value and the difference between the GP and the HOT traffic densities.[8]

Using the link numeration from Figure 2.5, the portion $\rho(t)$ of LOVs ready to pay toll $\pi\left(f_{22}^{in}(t)\right)$ in link 1 at time t is:

$$\rho(t) = \frac{1}{1+e^{-z(t)}}, \quad \text{where } z(t) = \alpha_0 + \alpha_1 \sum_{c=1}^{C} \left(\frac{n_2^c(t)}{L_2} - \frac{n_{22}^c(t)}{L_{22}} \right) + \alpha_2 \pi\left(f_{22}^{in}(t)\right). \tag{2.4.2}$$

[8]We did not include travel time and travel time reliability, because the analysis of I-10 East and West HOT lane data showed that there are always paying LOVs in the HOT lane, even during time periods when GP lane is *always* in free flow.

Here, $n_2^c(t)$, $n_{22}^c(t)$ are the vehicle counts in links 2 and 22 from Figure 2.5, respectivly; L_2, L_{22} are lane counts in those links; and $\alpha_0, \alpha_1, \alpha_2$ are known coefficients determined through calibration of the HOT controller (see Section 2.7.4).

Given the vehicle counts per commodity $n_1^c(t)$ and $n_{111}^c(t)$, $c = 1 \ldots, C$, and the portion of LOVs ready to pay $\rho(t)$, the HOT controller adjusts commodity counts as follows:

$$\tilde{n}_1^1(t) = (1 - \rho(t)) \left(n_1^1(t) + n_1^3(t)\right), \qquad \tilde{n}_1^3(t) = \rho(t) \left(n_1^1(t) + n_1^3(t)\right); \tag{2.4.3}$$

$$\tilde{n}_{111}^1(t) = (1 - \rho(t)) \left(n_{111}^1(t) + n_{111}^3(t)\right), \quad \tilde{n}_{111}^3(t) = \rho(t) \left(n_{111}^1(t) + n_{111}^3(t)\right). \tag{2.4.4}$$

Here, the link IDs refer to the configuration in Figure 2.5. We do not adjust commodities in the HOT link 11, because only ready to pay LOVs may be there.[9]

Now we can summarize the action of the HOT controller:

1. Determine toll π from the flow-price curve in Figure 2.6.
2. Compute $\rho(t)$ using formula (2.4.2).
3. Adjust commodity counts using formulae (2.4.3)-(2.4.4).

The HOT controller works on all GP links and on-ramps whose end node is a gate (in full access configuration, every node is a gate). This controller is activated in the step 2 of the simulation algorithm (see Section 2.2). Not all ready to pay vehicles end up in the HOT lane, but only those assigned to it in step 5 (split ratio assignment) of the simulation algorithm.

The case study with the HOT lane is presented in Section 3.3.

[9] Existing HOT policies are such that once a vehicle enters the HOT lane, its toll is set, and it is guaranteed that the driver would not be charged more than that. Thus, we can assume that those LOVs that were ready to pay and ended up in the HOT lane will stay ready to pay.

2.5 Input Data

The simulation input consists of:

- Road network description;
- Model parameters, i.e. link capacities, free flow speed and congestion wave speed values;
- Controllers defined by their parameters, e.g. HOT controllers;
- On- and off-ramp flows.

The first sheet of the Excel spreadsheet mentioned in Section 2.1 is called *Configuration*. It contains the descripttion of the road network and the model parameters, and its snapshot is presented in Figure 2.7.

In this particular case, in row 7 the node with ID 914827184 is a gate, where traffic can switch between the GP and the HOV/T lane. It has one incoming GP link 908310427 and two outgoing links: the GP link 908310428 and HOV/T link -908310428. As indicated by the corresponding parameter *Gate/Off-Ramps* in position D7, there are 4 off-ramps between this node and the next gate. In the case of the full access HOV/T lane, every node is a gate, and all instances of parameter *Gate/Off-Ramps* are set to 1. *Postmile* corresponds to the beginning of the link, and *Length (miles* shows link length.

Columns *Metered Lanes*, *Min Rate*, *Max Rate* and *OR Queue Limit* refer to a ramp metering policy, if such is present, and indicate, respectively, the number of metered lanes, the minimal metering rate per lane, the maximal metering rate per lane, and the number of vehicles the ramp can store before the spillback into the city streets occurs.

Parameter *OR Priority* indicates, whether traffic entering the freeway from the on-ramp has a merge priority over the mainline traffic. We shall discuss merge priorities in greater detail in Section 2.7.3.

HOT controllers are specified in the *HOT Control* sheet, shown in Figure 2.8. Figure 2.8. For each node that is a gate, we specify four time-varying parameters: coefficients $\alpha_0, \alpha_2, \alpha_3$ (rows 2-4

Road Network Description

	A	B	C	D	E	F	G	H	I	J	K
1	GP Link ID	HOV/T Link ID	Node ID	Gate/Off-Ramps	Postmile	Length (miles)	Detector	Layout	Aux Lanes	GP Lanes	HOV/T Lanes
2	908310422	0	914827179	0	9.44	0.178		|||||	0	5	0
3	908310423	0	914827180	0	9.62	0.178		|||||	0	5	0
4	908310424	0	914827181	0	9.80	0.178		|||||	0	5	0
5	908310425	0	914827182	0	9.97	0.178		|||||	0	5	0
6	908310426	0	914827183	0	10.15	0.178		|||||	0	5	0
7	908310427	0	914827184	4	10.33	0.178		|||||	0	5	0
8	908310428	-908310428	49322409	0	10.51	0.178		||||H	0	4	1
9	908310327	-908310327	914827120	0	10.69	0.168		/||||H	0	4	1
10	908310328	-908310328	49322578	0	10.85	0.168		\\\||||H	0	4	1
11	908310429	-908310429	914827185	0	11.02	0.172		||||H	0	4	1
12	908310430	-908310430	914827186	0	11.19	0.172		||||H	0	4	1

	P	Q	R	S	T	U	V	W	X	Y
1	On-Ramp ID	OR Lanes	Metered Lanes	Min Rate	Max Rate	OR Queue Limit	OR Priority	Off-Ramp ID	FR Lanes	Name
2	0	0	0			0	0	0	0	
3	0	0	0			0	0	0	0	
4	0	0	0			0	0	0	0	
5	0	0	0			0	0	0	0	
6	0	0	0			0	0	0	0	
7	0	0	0			0	0	0	0	
8	0	0	0			0	0	0	0	
9	0	0	0			0	0	-121240605	1	FR N. Figueroa St
10	0	0	0			0	0	0	0	
11	135273082	1	0			0	0	0	0	OR Colorado Blvd
12	0	0	0			0	0	0	0	

Model Parameters

	L	M	N	O
1	GP Cap. (vphl)	HOV/T Cap. (vphl)	FF Speed (mph)	C. Speed (mph)
2	1900	1800	65	25
3	1900	1800	65	25
4	1900	1800	65	25
5	1900	1800	65	25
6	1900	1800	66	16
7	1900	1800	66	16
8	1900	1800	66	16
9	1900	1800	66	16
10	1900	1800	66	16
11	1900	1800	66	16
12	1900	1800	66	16

Figure 2.7: Snapshot of the Configuration sheet.

in Figure 2.8) needed for equation (2.4.2); and the pointer to the pricing plan in the form of the spreadsheet cell identifier (row 5 in Figure 2.8). On the same sheet we specify pricing plans (see the bottom part of Figure 2.8). In our example, we have two pricing plans. Plan 1 (addressed as A140) is fixed: the price is constant — 25 cents per mile. Several fixed plans can be used to model time of day pricing. Plan 2 (addressed as C140) is dynamic: price is set based on the flow in the HOT lane, e.g. if the flow reaches $1,966$ vehicles per hour, the price per mile is set to 100 cents. Plan 1 is active during non-peak hours: from 0 to 5 am; from 9 am to 4 pm; and from 7 pm to 0 am. Plan 2 is activated during peak hours: from 5 to 9 am; and from 4 to 7 pm. In Figure 2.8, in row 5, one can see how the pricing plan changes at 9 am: at 8:55 the plan is 'C140' (dynamic), and

	A	B	C	DB	DC	DD	DE	DF	DG	DH	DI	DJ	DK	DL
1	**Node ID**	**Parameter**	0:00	8:35	8:40	8:45	8:50	8:55	9:00	9:05	9:10	9:15	9:20	9:25
2	914827184	alpha0	-0.6931	-0.6931	-0.6931	-0.6931	-0.6931	-0.6931	-0.6931	-0.6931	-0.6931	-0.6931	-0.6931	-0.6931
3	914827184	alpha1	0.0115	0.0115	0.0115	0.0115	0.0115	0.0115	0.0115	0.0115	0.0115	0.0115	0.0115	0.0115
4	914827184	alpha2	-0.0053	-0.0053	-0.0053	-0.0053	-0.0053	-0.0053	-0.0053	-0.0053	-0.0053	-0.0053	-0.0053	-0.0053
5	914827184	pricing plan	A140	C140	C140	C140	C140	C140	A140	A140	A140	A140	A140	A140

	A	B	C	D
138	**Plan 1**	**Plan 1**	**Plan 2**	**Plan 2**
139	**Flow (vph)**	**Price (cents)**	**Flow (vph)**	**Price (cents)**
140	0	25	585	35
141			651	40
142			724	45
143			804	50
144			890	55
145			983	60
146			1082	65
147			1188	70
148			1301	75
149			1421	80
150			1547	85
151			1680	90
152			1820	95
153			1966	100
154			2119	105
155			2279	110
156			2446	115
157			2619	120
158			2799	125
159			2985	130
160			3178	135
161			3378	140

Price per Mile Lookup Table

Figure 2.8: Snapshot of the HOT Control sheet — parameters for readiness to pay curve and references to pricing plans (top); fixed and dynamic pricing plans (bottom).

from 9:00 on, it is 'A140' (fixed).

The sheets *Collected On-Ramp Flows* and *Collected Off-Ramp Flows*, whose snapshots are presented in Figure 2.9, are used to enter the vehicle flows entering the freeway through on-ramps and exiting through off-ramps. These flows should be specified in vehicles-per-hour in 5-minute intervals. Thus, for a 24-hour period ramp would have 288 values specifying its flow. If the indicated flow exceeds ramp capacity, it will be capped at capacity.

Alternatively, off-ramp traffic can be specified through split ratios that specify portion of freeway traffic that must exist through off-ramps. These split ratios can be entered in the *Off-Ramp Split Ratios* sheet, whose snapshot is presented in the bottom of Figure 2.9. The simulation model described in Section 2.2 was originally designed to work with off-ramp split ratios, not flows. The main reason for that is that with split ratios traffic flow consistency is guaranteed, whereas the requested off-ramp flows may be larger than the mainline flow, and thus cannot be achieved. On

On-Ramp Flows

	A	B	C	D	E	F	G	H	I	J	K	FX	FY	FZ	GA	GB	GC	GD	GE	GF
1	GP Link ID	HOV/T Link ID	Postmile	Length (miles)	Detector	Ramp	Ramp ID	Layout	Name	Comments	0:00	14:05	14:10	14:15	14:20	14:25	14:30	14:35	14:40	14:45
2	908310422	0	9.44	0.178	0	0	908310422	|||||			1158	5812	5911	6036	6152	6211	6334	6394	6480	652
3	908310423	0	9.62	0.178	0	0	0	|||||			0	0	0	0	0	0	0	0	0	
4	908310424	0	9.80	0.178	0	0	0	|||||			0	0	0	0	0	0	0	0	0	
5	908310425	0	9.97	0.178	0	0	0	|||||			0	0	0	0	0	0	0	0	0	
6	908310426	0	10.15	0.178	0	0	0	|||||			0	0	0	0	0	0	0	0	0	
7	908310427	0	10.33	0.178	0	0	0	|||||			0	0	0	0	0	0	0	0	0	
8	908310428	-908310428	10.51	0.178	0	0	0	||||H			0	0	0	0	0	0	0	0	0	
9	908310327	-908310327	10.69	0.168	0	-1	0	/||||H	FR N. Figueroa St		0	0	0	0	0	0	0	0	0	
10	908310328	-908310328	10.85	0.168	0	0	0	||||H			0	0	0	0	0	0	0	0	0	
11	908310429	-908310429	11.02	0.172	0	1	135273082	||||H	OR Colorado Blvd	bad	34	278	232	300	237	233	301	300	300	2
12	908310430	-908310430	11.19	0.172	0	0	0	||||H			0	0	0	0	0	0	0	0	0	
13	908310431	-908310431	11.37	0.172	0	0	0	||||H			0	0	0	0	0	0	0	0	0	
14	908310365	-908310365	11.54	0.158	0	-1	0	/||||H	FR W Colorado Blvd		0	0	0	0	0	0	0	0	0	
15	908310366	-908310366	11.70	0.158	0	0	0	||||H			0	0	0	0	0	0	0	0	0	
16	908310432	-908310432	11.85	0.116	0	1	128794217	||||H	OR W Colorado Blvd		34	364	373	388	392	386	403	404	403	4
17	908310433	-908310433	11.97	0.116	0	0	0	||||H			0	0	0	0	0	0	0	0	0	

Off-Ramp Flows

	A	B	C	D	E	F	G	H	I	J	K	FX	FY	FZ	GA	GB	GC	GD	GE	GF
1	GP Link ID	HOV/T Link ID	Postmile	Length (miles)	Detector	Ramp	Ramp ID	Layout	Name	Comments	0:00	14:05	14:10	14:15	14:20	14:25	14:30	14:35	14:40	14:45
2	908310422	0	9.44	0.178	0	0	0	|||||			0	0	0	0	0	0	0	0	0	
3	908310423	0	9.62	0.178	0	0	0	|||||			0	0	0	0	0	0	0	0	0	
4	908310424	0	9.80	0.178	0	0	0	|||||			0	0	0	0	0	0	0	0	0	
5	908310425	0	9.97	0.178	0	0	0	|||||			0	0	0	0	0	0	0	0	0	
6	908310426	0	10.15	0.178	0	0	0	|||||			0	0	0	0	0	0	0	0	0	
7	908310427	0	10.33	0.178	0	0	0	|||||			0	0	0	0	0	0	0	0	0	
8	908310428	-908310428	10.51	0.178	0	0	0	||||H			0	0	0	0	0	0	0	0	0	
9	908310327	-908310327	10.69	0.168	0	-1	-121240605	/||||H	FR N. Figueroa St		34	235	247	256	262	250	257	247	252	2
10	908310328	-908310328	10.85	0.168	0	0	0	||||H			0	0	0	0	0	0	0	0	0	
11	908310429	-908310429	11.02	0.172	0	1	0	||||H	OR Colorado Blvd		0	0	0	0	0	0	0	0	0	
12	908310430	-908310430	11.19	0.172	0	0	0	||||H			0	0	0	0	0	0	0	0	0	
13	908310431	-908310431	11.37	0.172	0	0	0	||||H			0	0	0	0	0	0	0	0	0	
14	908310365	-908310365	11.54	0.158	0	-1	128794214	/||||H	FR W Colorado Blvd		6	37	43	45	44	47	46	41	43	
15	908310366	-908310366	11.70	0.158	0	0	0	||||H			0	0	0	0	0	0	0	0	0	
16	908310432	-908310432	11.85	0.116	0	1	0	||||H	OR W Colorado Blvd		0	0	0	0	0	0	0	0	0	
17	908310433	-908310433	11.97	0.116	0	0	0	||||H			0	0	0	0	0	0	0	0	0	

Off-Ramp Split Ratios

	A	B	C	D	E	F	G	H	I	J	K	FX	FY	FZ	GA	GB	GC	GD	GE	GF
1	GP Link ID	HOV/T Link ID	Postmile	Length (miles)	Detector	Ramp	Ramp ID	Layout	Name	Comments	0:00	14:05	14:10	14:15	14:20	14:25	14:30	14:35	14:40	14:45
2	908310422	0	9.44	0.178	0	0	0	|||||			0	0	0	0	0	0	0	0	0	
3	908310423	0	9.62	0.178	0	0	0	|||||			0	0	0	0	0	0	0	0	0	
4	908310424	0	9.80	0.178	0	0	0	|||||			0	0	0	0	0	0	0	0	0	
5	908310425	0	9.97	0.178	0	0	0	|||||			0	0	0	0	0	0	0	0	0	
6	908310426	0	10.15	0.178	0	0	0	|||||			0	0	0	0	0	0	0	0	0	
7	908310427	0	10.33	0.178	0	0	0	|||||			0	0	0	0	0	0	0	0	0	
8	908310428	-908310428	10.51	0.178	0	0	0	||||H			0	0	0	0	0	0	0	0	0	
9	908310327	-908310327	10.69	0.168	0	-1	-121240605	/||||H	FR N. Figueroa St		0.0273	0.0537	0.0547	0.0547	0.0488	0.0498	0.0469	0.0469	0.0444	0.04
10	908310328	-908310328	10.85	0.168	0	0	0	||||H			0	0	0	0	0	0	0	0	0	
11	908310429	-908310429	11.02	0.172	0	1	0	||||H	OR Colorado Blvd		0	0	0	0	0	0	0	0	0	
12	908310430	-908310430	11.19	0.172	0	0	0	||||H			0	0	0	0	0	0	0	0	0	
13	908310431	-908310431	11.37	0.172	0	0	0	||||H			0	0	0	0	0	0	0	0	0	
14	908310365	-908310365	11.54	0.158	0	-1	128794214	/||||H	FR W Colorado Blvd		0.0044	0.0093	0.0093	0.0093	0.0093	0.0088	0.0073	0.0083	0.0083	0.00
15	908310366	-908310366	11.70	0.158	0	0	0	||||H			0	0	0	0	0	0	0	0	0	
16	908310432	-908310432	11.85	0.116	0	1	0	||||H	OR W Colorado Blvd		0	0	0	0	0	0	0	0	0	
17	908310433	-908310433	11.97	0.116	0	0	0	||||H			0	0	0	0	0	0	0	0	0	

Figure 2.9: Snapshots of the Collected On-Ramp Flows sheet (top), Collected Off-Ramp Flows sheet (middle) and Off-Ramp Split Ratios sheet (bottom).

the other hand, off-ramp vehicle flows can be measured directly, whereas split ratios can only be estimated. The methodology for estimating off-ramp split ratios is discussed in Sections 2.7.6 and 2.7.7.

Lastly, we need to specify the portion of the HOV traffic in on-ramp flows that enter the system. This is done in the *HOV Portion* sheet, shown in Figure 2.10. For each on-ramp, the HOV traffic portion is specified by the nonnegative number between 0 and 1 in 5-minute intervals, which makes it 288 values for a 24-hour simulation.

	A	B	C	D	E	F	G	H	I	J	K	FX	FY	FZ	GA	GB	GC	GD	GE	GF
1	GP Link ID	HOV Link ID	Postmile	Length (miles)	Detector	Ramp	Ramp ID	Layout	Name	Comments	0:00	14:05	14:10	14:15	14:20	14:25	14:30	14:35	14:40	14:45
2	908310422	0	9.44	0.178	0	0	908310422	IIIII			0.15	0.25	0.25	0.25	0.25	0.25	0.25	0.25	0.25	0.2
3	908310423	0	9.62	0.178	0	0	0	IIIII			0	0	0	0	0	0	0	0	0	
4	908310424	0	9.80	0.178	0	0	0	IIIII			0	0	0	0	0	0	0	0	0	
5	908310425	0	9.97	0.178	0	0	0	IIIII			0	0	0	0	0	0	0	0	0	
6	908310426	0	10.15	0.178	0	0	0	IIIII			0	0	0	0	0	0	0	0	0	
7	908310427	0	10.33	0.178	0	0	0	IIIII		HOV Gate	0	0	0	0	0	0	0	0	0	
8	908310428	-908310428	10.51	0.178	0	0	0	IIIIIH			0	0	0	0	0	0	0	0	0	
9	908310327	-908310327	10.69	0.168	0	-1	0	IIIIIH	FR N. Figueroa St		0	0	0	0	0	0	0	0	0	
10	908310328	-908310328	10.85	0.168	0	0	0	IIIIIH			0	0	0	0	0	0	0	0	0	
11	908310429	-908310429	11.02	0.172	0	1	135273082	IIIIIH	OR Colorado Blvd	End HOV Gate	0.15	0.25	0.25	0.25	0.25	0.25	0.25	0.25	0.25	0.2
12	908310430	-908310430	11.19	0.172	0	0	0	IIIIIH			0	0	0	0	0	0	0	0	0	
13	908310431	-908310431	11.37	0.172	0	0	0	IIIIIH			0	0	0	0	0	0	0	0	0	
14	908310365	-908310365	11.54	0.158	0	-1	0	IIIIIH	FR W Colorado Blvd		0	0	0	0	0	0	0	0	0	
15	908310366	-908310366	11.70	0.158	0	0	0	IIIIIH			0	0	0	0	0	0	0	0	0	
16	908310432	-908310432	11.85	0.116	0	1	128794217	IIIIIH	OR W Colorado Blvd		0.15	0.25	0.25	0.25	0.25	0.25	0.25	0.25	0.25	0.2
17	908310433	-908310433	11.97	0.116	0	0	0	IIIIIH			0	0	0	0	0	0	0	0	0	

Figure 2.10: Snapshot of the HOV Portion sheet.

2.6 Simulation Output and Reporting

The simulation produces the following output:

- **Vehicle density** in GP and HOV/T links, averaged over 5-minute intervals and reported in vehicles per mile. Figure 2.11 presents the snapshots of *GP Density* and *HOV/T Density* sheets containing the density values. All othersimulation mentioned in this Section are presented in a similar way.

- **Flow** entering GP and HOV/T links aggregated in 5-minute intervals and reported in *GP Flow* and *HOV/T Flow* sheets in vehicles per hour.

- **Speed** in GP and HOV/T links averaged over 5-minute intervals and reported in *GP Speed* and *HOV/T Speed* sheets in miles per hour.

From these data the following performance measures are computed:

- **On-ramp queues**. An on-ramp accumulates a queue when its demand exceeds the flow this on-ramp actually sends to the freeway. There are 3 cases, when this may happen:

  (1) demand exceeds on-ramp capacity;

  (2) not all the vehicles desiring to enter freeway can be satisfied due to congestion in the mainlines; and

  (3) ramp metering is on, and vehicles accumulate at the on-ramp.

GP Density

	A	B	C	D	E	F	G	H	I	FV	FW	FX	FY	FZ	GA	GB	GC	GD
1	GP Link ID	PM	Length (miles)	Detector	Cr. Density (vpm)	Layout	Name	Comments	0:00	14:05	14:10	14:15	14:20	14:25	14:30	14:35	14:40	14:45
2	908310422	9.44	0.178	0	129	IIIII			0	0	0	0	0	0	0	0	0	0
3	908310423	9.62	0.178	0	129	IIIII			17	85	86	88	94	96	97	98	100	100
4	908310424	9.80	0.178	0	129	IIIII			16	85	86	88	94	95	97	98	100	100
5	908310425	9.97	0.178	0	129	IIIII			16	85	86	88	94	95	97	98	100	100
6	908310426	10.15	0.178	0	115	IIIII			15	83	85	87	92	94	96	97	98	99
7	908310427	10.33	0.178	0	115	IIIII			12	70	71	72	77	78	80	81	82	82
8	908310428	10.51	0.178	0	115	IIIIIH			12	69	71	72	77	78	80	81	82	82
9	908310327	10.69	0.168	0	115	/IIIIH	FR N. Figueroa St		11	66	67	68	73	74	76	77	78	79
10	908310328	10.85	0.168	0	115	\IIIIH			11	66	67	68	72	74	76	77	78	79
11	908310429	11.02	0.172	0	115	IIIIIH	OR Colorado Blvd		11	70	71	73	77	79	80	81	82	83
12	908310430	11.19	0.172	0	115	IIIIIH			10	70	71	73	77	79	80	81	82	83
13	908310431	11.37	0.172	0	133	IIIIIH			10	70	71	72	76	79	80	81	82	83
14	908310365	11.54	0.158	0	133	/IIIIH	FR W Colorado Blvd		9	69	70	72	76	78	80	81	82	82
15	908310366	11.70	0.158	0	133	\IIIIH			9	69	70	72	75	78	80	81	82	82
16	908310432	11.85	0.116	0	166	IIIIIH	OR W Colorado Blvd		9	75	76	78	81	84	86	87	88	89
17	908310433	11.97	0.116	0	166	IIIIIH			9	75	76	77	81	84	86	87	88	89

HOV/T Density

	A	B	C	D	E	F	G	H	I	FV	FW	FX	FY	FZ	GA	GB	GC	GD
1	HOV/T Link ID	PM	Length (miles)	Detector	Cr. Density (vpm)	Layout	Name	Comments	0:00	14:05	14:10	14:15	14:20	14:25	14:30	14:35	14:40	14:45
2	0	9.44	0.178	0	28	IIIII			0	0	0	0	0	0	0	0	0	0
3	0	9.62	0.178	0	28	IIIII			0	0	0	0	0	0	0	0	0	0
4	0	9.80	0.178	0	28	IIIII			0	0	0	0	0	0	0	0	0	0
5	0	9.97	0.178	0	28	IIIII			0	0	0	0	0	0	0	0	0	0
6	0	10.15	0.178	0	27	IIIII			0	0	0	0	0	0	0	0	0	0
7	0	10.33	0.178	0	27	IIIII		HOV Gate	2	14	14	14	15	16	16	16	16	16
8	-908310428	10.51	0.178	0	27	IIIIIH			2	14	14	14	15	16	16	16	16	16
9	-908310327	10.69	0.168	0	27	/IIIIH	FR N. Figueroa St		2	14	14	14	15	16	16	16	16	16
10	-908310328	10.85	0.168	0	27	\IIIIH			2	14	14	14	15	16	16	16	16	16
11	-908310429	11.02	0.172	0	27	IIIIIH	OR Colorado Blvd	End HOV Gate	2	14	14	14	15	16	16	16	16	16
12	-908310430	11.19	0.172	0	27	IIIIIH			2	14	14	14	15	16	16	16	16	16
13	-908310431	11.37	0.172	0	27	IIIIIH			2	14	14	14	15	16	16	16	16	16
14	-908310365	11.54	0.158	0	27	/IIIIH	FR W Colorado Blvd		2	14	14	14	15	16	16	16	16	16
15	-908310366	11.70	0.158	0	27	\IIIIH			2	14	14	14	15	16	16	16	16	16
16	-908310432	11.85	0.116	0	27	IIIIIH	OR W Colorado Blvd		1	14	14	14	15	16	16	16	16	16
17	-908310433	11.97	0.116	0	27	IIIIIH			1	14	14	14	15	16	16	16	16	16

Figure 2.11: Snapshots of the GP Density sheet (top) and HOV/T Density sheet (bottom).

If the on-ramp queue is non-empty, the on-ramp tries sending all the vehicles in the queue, plus the demand to the freeway. Thus, the on-ramp out-flow can exceed demand, in which case the queue decreases. The average queue dynamics follows the formula:

$$q_l(t + \Delta t) = \max\left\{0, q_l(t) + \left(d_l(t) - f_l^{out}(t)\right)\Delta t\right\} \tag{2.6.1}$$

where $q_l(t)$ represents the queue size in the on-ramp link l, $d_l(t)$ is the demand — the flow desiring to enter the freeway, $f_l^{out}(t)$ is the actual flow leaving the on-ramp, and Δt is the size of the aggregation time interval. On-ramp queues averaged over 5-minute intervals ($\Delta t = 5$ minutes) are reported in the *On-Ramp Queue* sheet.

- **Vehicle Miles Traveled (VMT)** in each GP and HOV/T link l:

$$\text{VMT}_l(t) = f_l^{out}(t)\Delta x_l \Delta t, \tag{2.6.2}$$

where $f_l^{out}(t)$ is the total flow leaving link l at time t, and Δx_l is the length of link l. For on-ramp links, $\text{VMT}_l(t) = 0$. VMT values, aggregated in 5-minute intervals, are reported in in the *GP VMT* sheet for GP links and in the *HOV/T VMT* sheet for HOV/T links.

- **Vehicle Hours Traveled (VHT)** in each link l. For ordinary GP and HOV/T links,

$$\text{VHT}_l(t) = n(t)\Delta x_l \Delta t, \tag{2.6.3}$$

where $n(t)$ is the total vehicle density in l at time t, given in vehicles per mile. For each on-ramps,

$$\text{OR-VHT}_l(t) = q_l(t)\Delta t, \tag{2.6.4}$$

where $q_l(t)$ is the size of queue at the on-ramp l at time t. GP and HOV/T VHT values, aggregated in 5-minute intervals, are reported in in the *GP VHT* sheet for GP links and in the *HOV/T VHT* sheet for HOV/T links. Total VHT, composed of GP, HOV/T and on-ramp VHT, aggregated in 5-minute intervals, is reported in the *Total VHT* sheet.

- **Delay** in each link l. For ordinary GP and HOV/T links,

$$\text{Delay}_l(t) = \text{VHT}_l(t) - \frac{\text{VMT}_l(t)}{v_l}, \tag{2.6.5}$$

where v_l is the free flow speed in link l.[10] For on-ramps,

$$\text{OR-Delay}_l(t) = \text{OR-VHT}_l(t). \tag{2.6.6}$$

GP and HOV/T delay values, aggregated in 5-minute intervals, are reported in in the *GP Delay* sheet for GP links and in the *HOV/T Delay* sheet for HOV/T links. Total delay, composed of GP, HOV/T and on-ramp delay, aggregated in 5-minute intervals, is reported in the *Total Delay* sheet.

2.7 Model Calibration

When it comes to the simulation of real world traffic networks, in our case freeways with HOV/T lanes, the quality of the simulation results is assessed by comparing them with detector measure-

[10] Instead of v_l, we could use other reference speed values, e.g. 45 or 60 mph.

ments. We expect to have flow and speed measurements at the freeway mainline (from both GP and HOV/T lanes), as well as flow measurements at on- and off-ramps. To better match the detector measurements the simulation model needs to be tuned. Tunable parameters of our model are:

- Fundamental diagram for each link;
- Percentage of HOVs in the traffic flow entering the system;
- Input link priorities in nodes with multiple inputs;
- HOT controller;
- On- and off-ramp flows;
- Off-ramp split ratios that are computed differently for the full access and separated HOV/T facilities.

Next, we discuss calibration of each of these items in more detail.

2.7.1 Fundamental Diagrams

Traffic flow parameters governing the simulation model are defined by:

- free flow speed, v_l^f;
- congestion wave speed, w_l;
- capacity or maximum flow, F_l; and
- jam density, n_l^J.

These parameters are referred to as the *fundamental diagram* and are assigned to each link. Here, capacity is the most significant parameter, as it ultimately determines the location of bottlenecks in space and time. The model is very sensitive to capacity variations. The second significant parameter is the free flow speed, which affects the intensity of uncongested traffic. The model is

quite sensitive to free flow speed variations. The least significant parameter is the congestion wave speed. If a given link gets congested, the congestion wave speed determines how fast congestion would propagate upstream of this link. The model is not very sensitive to congestion wave speed variations. Finally, under the assumption that when traffic is queued up and standing still, each vehicle takes up 26 feet, the jam density can be set to $n_l^J = 200$ vpml. Alternatively, one may assume the fundamental diagram is of triangular shape. Then,

$$n_l^J = \frac{F_l}{v_l^f} + \frac{F_l}{w_l}.$$

For those links with healthy loop detection and where traffic flow reaches maximum at some point during the day, fundamental diagrams can be inferred from loop data. Figure 2.12 presents an estimation of the fundamental diagram from loop data. Two cases are shown:

(a) good data that allow estimating all three parameters, free flow speed, capacity and congestion wave speed; and

(b) data sufficient only for the free flow speed estimation.

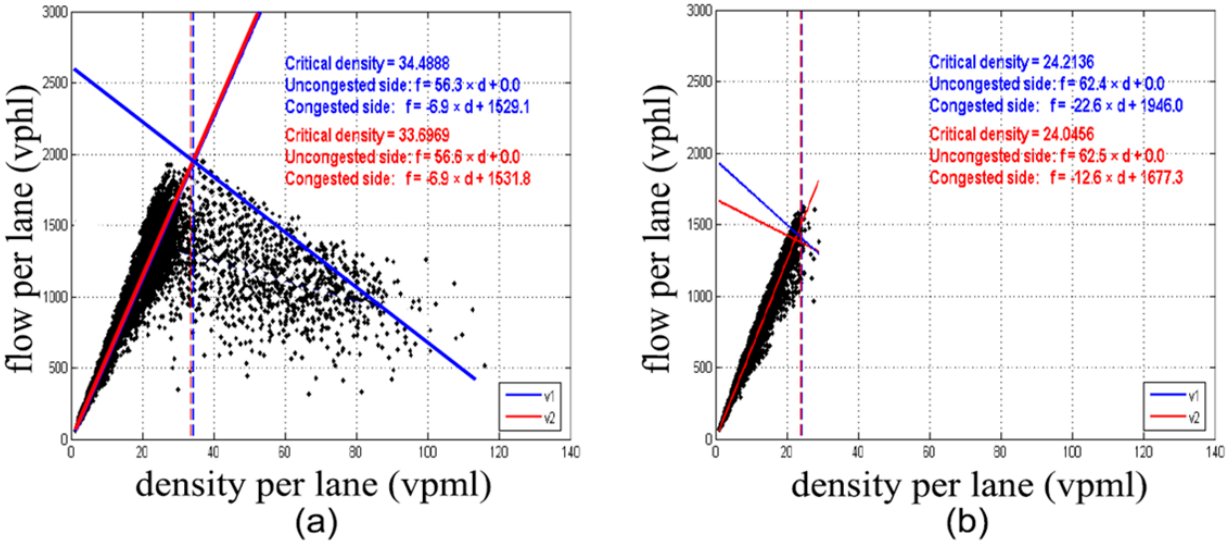

Figure 2.12: Estimation of the fundamental diagram from measurement data — (a) good data; (b) bad data.

Calibration of the fundamental diagram is typically model-agnostic, and there exists an abundant research on this topic, including from some of the authors of this report, e.g. [8]. Fundamental diagrams obtained from measurement data must go through a sanity check:

1. Capacity values should be in the range from 1,800 to 2,200 vphl for GP lanes and in the range from 1,600 to 1,800 vphl for HOV/T lanes;
2. Free flow speed values should be in the range from 55 to 70 mph;
3. Congestion wave speed values should be in the range from 10 to 20 mph.

Generally, PeMS [5] is used as a rich source of freeway traffic data: it provides occupancy, flow and speed at detector locations and identifies bottlenecks. From there we can learn whether a particular detector is always in free flow, near a bottleneck, or in the middle of a bottleneck queue.

Links without loop detection can either borrow fundamental diagrams from their upstream or downstream neighbors, if those neighbors have data, or use the default values.

If traffic measurements are not available for the fundamental diagram estimation, or the sanity check failed, default values from Table 2.1 are used.

	GP Lane	Auxiliary Lane	HOV/T Lane
Free Flow Speed	65 mph	65 mph	65 mph
Congestion Wave Speed	15 mph	15 mph	15 mph
Capacity	1,900 vphl	900 vphl	1600 vphl
Jam Density	200 vpml	200 vpml	200 vpml

Table 2.1: Default values for the fundamental diagram.

2.7.2 Portion of HOVs in On-Ramp Demand

This parameter generally depends on the time of day and location as well as on the type of HOV/T lane.[11] Presently, we do not have a rigorous methodology for accurate estimation of the HOV portion of traffic entering the freeway.

[11]Typical minimum vehicle occupancy level for HOV lanes in the U.S. is 2 (2+HOV) or sometimes 3 (3+HOV).

The simple approach would be to assign the ratio of the HOV lane vehicle count to the total freeway vehicle count during periods of congestion at any given location as the HOV portion of traffic.

2.7.3 Input Link Priorities

To illustrate the role of priorities, let us discuss how flows are computed at a merge node, where an on-ramp enters the freeway. Consider the example, shown in Figure 2.13: flows from links 1 and 2, S_1 and S_2, with priorities p_1 and p_2, merge into link 3, which can accept flow R_3.

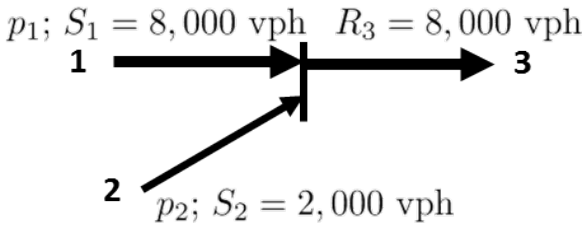

Figure 2.13: Merge node example.

The case when $S_1 + S_2 \leq R_3$ is trivial: both flows can be accepted by link 3 without modification. However, if $S_1 + S_2 > R_3$ (as in Figure 2.13), the actual flows coming out of links 1 and 2, f_1^{out} and f_2^{out}, are scaled down versions of S_1 and S_2:

$$\begin{aligned} f_1^{out} &= \min\left\{S_1,\ \max\left\{\frac{p_1}{p_1+p_2}R_3,\ R_3 - S_2\right\}\right\}; \\ f_2^{out} &= \min\left\{S_2,\ \max\left\{\frac{p_2}{p_1+p_2}R_3,\ R_3 - S_1\right\}\right\}. \end{aligned}$$

Choice of priorities defines the upstream direction of congestion propagation. If $p_1 = \frac{S_1}{S1+S_2} = \frac{4}{5}$ and $p_2 = \frac{S_2}{S_1+S_2} = \frac{1}{5}$, then $f_1^{out} = 6,400$ vph and $f_2^{out} = 1,600$ vph. On the other hand, if $p_1 = 0$ and $p_2 = 1$, then $f_1^{out} = 6,000$ vph and $f_2^{out} = 2,000$ vph.

We recommend making link priorities *proportional to link capacities.*

2.7.4 HOT Controller

To compute coefficients $\alpha_0, \alpha_1, \alpha_2$ for the formula (2.4.2), we make the following assumptions:

1. We can count vehicles in the GP lane, $\hat{n}^t_{GP}$, and in the HOT lane, $\hat{n}^t_{HOT}$ at any given time t.

2. We have data to estimate the LOV traffic portion ready to pay at time t, $\hat{\rho}^t$:

$$\hat{\rho}^t = \frac{\text{Number of LOVs in the HOT link at time } t}{\text{Total number of LOVs in both HOT and GP links at time } t}. \tag{2.7.1}$$

   The nominator in the right hand side of this formula comes from FasTrak data collected in the HOT lane — if the vehicle pays, it is LOV, otherwise it is HOV. The denominator in the right hand side of this formula is computed as a sum of vehicle count in the GP lane, which can be obtained from PeMS [5], and the number of LOVs in the HOT lane. Obviously, $\hat{\rho} \in [0, 1]$.

3. We know HOT price per mile at time t, π^t, which comes from the FasTrak toll logs.

4. If traffic density per lane in the GP and the HOT lanes were the same and no tolls were collected, we assume the readiness to pay $\rho = \frac{L_{HOT}}{L_{GP}+L_{HOT}}$, where L_{GP} and L_{HOT} denote lane counts in GP and HOT links (links 2 and 22 from Figure 2.5 respectively). According to (2.4.2),

$$\rho = \frac{1}{1+e^{-\alpha_0}} = \frac{e^{\alpha_0}}{1+e^{\alpha_0}} = \frac{L_{HOT}}{L_{GP}+L_{HOT}}. \tag{2.7.2}$$

   Hence,

$$\alpha_0 = \ln\left(\frac{\rho}{1-\rho}\right) = \ln\left(\frac{L_{HOT}}{L_{GP}}\right). \tag{2.7.3}$$

   Thus, it remains to determine coefficients α_1 and α_2.

We will estimate α_1, α_2 from equations:

$$\ln\left(\frac{\hat{\rho}^t}{1-\hat{\rho}^t}\right) = \ln\left(\frac{L_{HOT}}{L_{GP}}\right) + \alpha_1\left(\frac{\hat{n}^t_{GP}}{L_{GP}} - \frac{\hat{n}^t_{HOT}}{L_{HOT}}\right) + \alpha_2\pi^t, \quad t = 1, \ldots, \Theta. \tag{2.7.4}$$

Denote:

$$\boldsymbol{X} = \begin{pmatrix} \frac{\hat{n}^1_{GP}}{L_{GP}} - \frac{\hat{n}^1_{HOT}}{L_{HOT}} & \pi^1 \\ \dots & \dots \\ \frac{\hat{n}^\Theta_{GP}}{L_{GP}} - \frac{\hat{n}^\Theta_{HOT}}{L_{HOT}} & \pi^\Theta \end{pmatrix}, \quad \text{and} \quad \boldsymbol{Y} = \begin{pmatrix} \ln\left(\frac{\hat{\rho}^1}{1-\hat{\rho}^1}\right) - \ln\left(\frac{L_{HOT}}{L_{GP}}\right) \\ \vdots \\ \ln\left(\frac{\hat{\rho}^\Theta}{1-\hat{\rho}^\Theta}\right) - \ln\left(\frac{L_{HOT}}{L_{GP}}\right) \end{pmatrix}. \tag{2.7.5}$$

Equations (2.7.4) can be rewritten as:

$$\boldsymbol{Y} = \boldsymbol{X} \begin{pmatrix} \alpha_1 \\ \alpha_2 \end{pmatrix}. \tag{2.7.6}$$

Thus, α_1, α_2 can be estimated using the least squares method:

$$\begin{pmatrix} \alpha_1 \\ \alpha_2 \end{pmatrix} = \left(\boldsymbol{X}^T \boldsymbol{X}\right)^{-1} \boldsymbol{X}^T \boldsymbol{Y}. \tag{2.7.7}$$

2.7.5 Ramp Flows

Vehicle counts for the first freeway link (mainline entry), on-ramps and off-ramps must be obtained. Possible sources of these data are: PeMS, Census counts and manual counts collected for the given, previous or related freeway corridor studies. Data sets for the mainline entry point and each of the ramps should be processed as follows:

1. Use only weekday counts, excluding Fridays and holidays, to find the average flow profile;
2. Use 5-minute flow profile if readily available; otherwise produce 5-minute flow profile from the hourly profile by interpolating, as shown in Figure 2.14.

Recall from Section 2.5 that the model input are 5-minute demand values, but our initial data are collected 5-minute ramp flows. To retain the knowledge of the original ramp flows and to keep track of the tuning process — that is, to be able to see how significantly do we change the original ramp

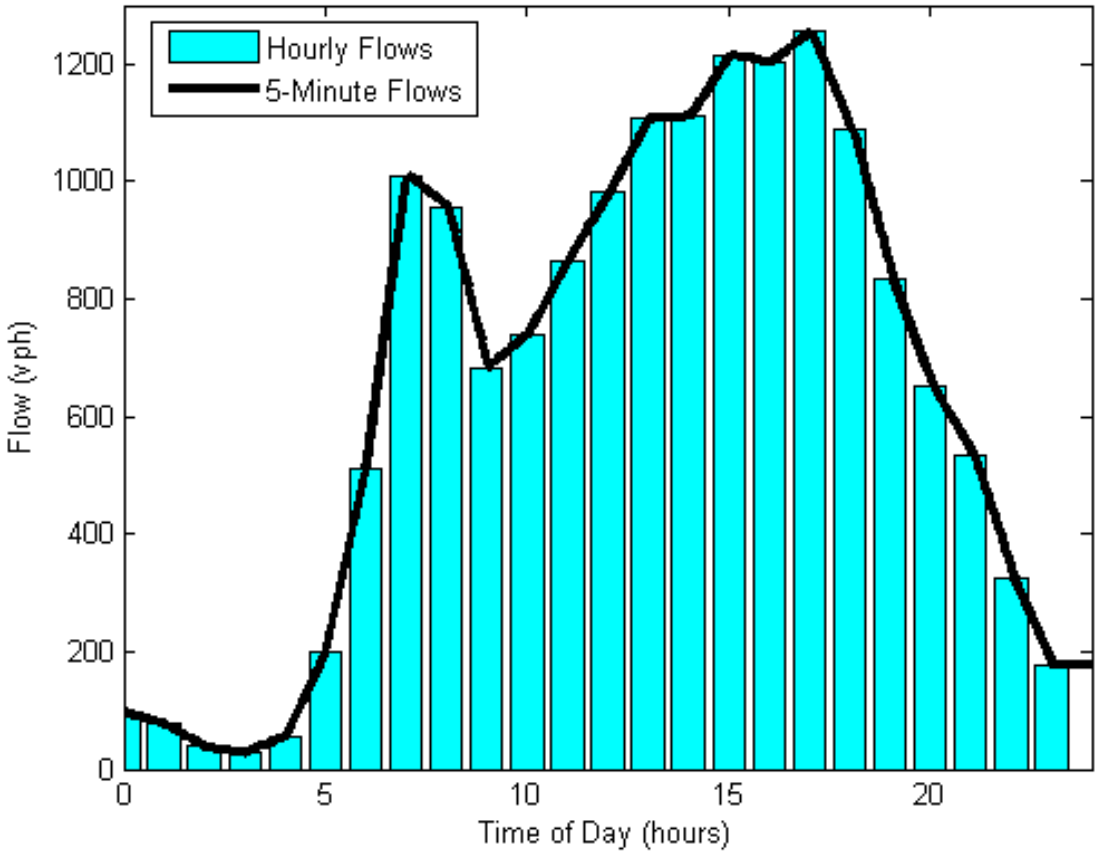

Figure 2.14: Generating 5-minute flow profile from hourly vehicle counts.

flow — we introduce *knobs*. Knobs are coefficients, by which we multiply original flows to obtain demand values that go into the model as input data. So, for the mainline, on- or off-ramp demand at time t is:

$$d_l(t) = \text{Knob}_l(t) \times \text{CollectedFlow}_l(t).$$

Obviously, the first freeway link, every on- and off-ramp, each has its own set of 288 knobs — one knob per 5-minute interval. Knobs can be found in the *On-Ramp Knobs* and *Off-Ramp Knobs* sheets of the spreadsheet. As their names suggest, the first is used with on-ramp and the second one — with off-ramp flows.

Initially, all knobs are set to 1 — that is, collected flows are fed to the model unchanged. Then, we start tweaking the knobs. For example, $\text{knob}_l = 1.1$ increases the original flow of ramp link l by 10%, whereas $\text{knob}_l = 0.9$ decreases the original flow of ramp link l by 10%.

Note: It may be a requirement for the calibrated model input to be as close to the collected flows as possible, e.g. to be within ±15%. Then, the admissible interval for knob values is from 0.85 to 1.15. Typically, the variation of off-ramp knobs is less restrictive than that of on-ramp knobs.

The knob tuning process is a repetition of three actions until the simulation produces the expected congestion pattern:

1. change knob values;
2. run simulation;
3. inspect the resulting congestion pattern.

The general approach to model calibration through demand adjustment can be described as follows:

1. Tune off-ramp knobs so that the simulation produces free flow traffic pattern — that is, if there is any congestion, remove it by increasing knobs for off-ramps upstream of any bottleneck;
2. Sort the bottlenecks from the expected congestion pattern by time of activation, then by location from upstream to downstream;
3. For each bottleneck in the list, find the relevant ramps that control this bottleneck — these are ramps between the current bottleneck and the nearest active upstream bottleneck, or if such does not exist, the beginning of the freeway corridor;
4. For each bottleneck, first decrease the relevant off-ramp knobs, then, if necessary, increase the relevant on-ramp knobs, to achieve the expected bottleneck behavior in terms of its activation time, duration and resulting queue;
5. Once the simulation produces the result close enough to the expected congestion pattern, save the off-ramp split ratios — in scenario modeling, the split ratios will define the off-ramp demand.

Knobs can be tweaked in chunks of arbitrary size (between 1 and 288). Intelligent knob tuning requires some calculations on the part of the modeler. For instance, to activate a bottleneck the sum of all incoming flows minus all outgoing flows upstream of the bottleneck should exceed freeway capacity at the bottleneck location. On the other hand, if one wishes to avoid bottleneck activation at a given location at a given time, one must ensure that the total net flow leading to this location at this time is below the freeway capacity at this location.

2.7.6 Split Ratios for the Full Access HOV/T Lane

Consider a node, one of whose output links is an off-ramp, depicted in Figure 2.5. We shall make the following assumptions.

1. Total flow entering the off-ramp, $\hat{f}^{in}_{222}$, at any given time is known (from measurements) and is not restricted by the off-ramp supply: $\hat{f}^{in}_{222} < R_{222}$.

2. Portions of traffic sent to the off-ramp from the HOV/T lane and from the GP lane at any given time are equal: $\beta^c_{1,222} = \beta^c_{11,222} = \beta$, $c = 1, \ldots, C$.

3. None of the flow coming from the on-ramp (link 111), if such flow exists, is directed toward the off-ramp. In other words, $\beta^c_{111,222} = 0$, $c = 1, \ldots, C$.

4. Distribution of flow portions not directed to the off-ramp between the HOV/T and the GP output links is known. This can be written as: $\beta^c_{ij} = (1 - \beta)\delta^c_{ij}$, where $\delta^c_{ij} \in [0, 1]$, as well as $\beta_{111,j}$, $i = 1, 11$, $j = 2, 22$, $c = 1, \ldots, C$, are known.

5. Demand S^c_i, $i = 1, 11, 111$, $c = 1, \ldots, C$, and supply R_j, $j = 2, 22$, are given.

At any given time, β is unknown and is to be found.

If β were known, the node model, described in step 6 of the simulation model (Section 2.2, would compute the input-output flows, in particular, $f_{i,222} = \sum_{c=1}^{C} f^c_{i,222}$, $i = 1, 11$. Define

$$\psi(\beta) = f_{1,222} + f_{11,222} - \hat{f}^{in}_{222}. \tag{2.7.8}$$

Our goal is to find β from the equation:

$$\psi(\beta) = 0, \tag{2.7.9}$$

such that $\beta \in \left[\frac{\hat{f}_{222}^{in}}{S_1+S_{11}}, 1\right]$, where $S_i = \sum_{c=1}^{C} S_i^c$. Obviously, if $S_1 + S_{11} < \hat{f}_{222}^{in}$, the solution does not exist, and the best we can do in this case, is to set $\beta = 1$ directing all traffic from links 1 and 11 to the off-ramp.

Suppose now that $S_1 + S_{11} >= \hat{f}_{222}^{in}$. For any given $\hat{f}_{222}^{in}$, $\psi(\beta)$ is a monotonically increasing function of β. Moreover, $\psi\left(\frac{\hat{f}_{222}^{in}}{S_1+S_{11}}\right) \leq 0$, while $\psi(1) \geq 0$. Thus, the solution of (2.7.9) within given interval exists and can be obtained using the *bisection method*.

The algorithm for finding β follows.

1. Initialize:

$$\begin{aligned} \underline{b}(0) &:= \frac{\hat{f}_{222}^{in}}{S_1 + S_{11}}; \\ \overline{b}(0) &:= 1; \\ k &:= 0. \end{aligned}$$

2. If $S_1 + S_{11} \leq \hat{f}_{222}^{in}$, then set $\beta = 1$ and stop.

3. Run the node model from step 6 of the simulation model (Section 2.2) with $\beta = \underline{b}(0)$ and evaluate $\psi(\beta)$. If $\psi(\underline{b}(0)) \geq 0$, then set $\beta = \underline{b}(0)$ and stop.

4. Run the node model from step 6 of the simulation model (Section 2.2) with $\beta = \frac{\underline{b}(k)+\overline{b}(k)}{2}$ and evaluate $\psi(\beta)$. If $\psi\left(\frac{\underline{b}(k)+\overline{b}(k)}{2}\right) = 0$, then set $\beta = \frac{\underline{b}(k)+\overline{b}(k)}{2}$ and stop.

5. If $\psi\left(\frac{\underline{b}(k)+\overline{b}(k)}{2}\right) < 0$, then update:

$$\begin{aligned} \underline{b}(k+1) &= \frac{\underline{b}(k) + \overline{b}(k)}{2}; \\ \overline{b}(k+1) &= \overline{b}(k). \end{aligned}$$

Else, update:

$$\begin{aligned} \underline{b}(k+1) &= \underline{b}(k); \\ \overline{b}(k+1) &= \frac{\underline{b}(k)+\overline{b}(k)}{2}. \end{aligned}$$

6. Set $k := k+1$ and return to step 4.

2.7.7 Split Ratios for the Limited Access HOV/T Lane

The configuration of a node with an off-ramp as one of the output links is simpler in the case of a limited access HOV/T lane, as shown in Figure 2.15. Here, traffic cannot directly go from the HOV/T lane to link 222, and, thus, we have to deal only with the 2-input-2-output node. There is a caveat, however. Recall from Section 2.3.2 that in the separate HOV/T lane case we have destination-based traffic commodities, and split ratios for destination-based traffic are fixed.

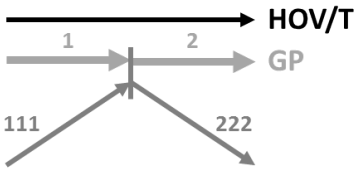

Figure 2.15: A node with a GP link and an on-ramp as inputs, and a GP link and an off-ramp as outputs.

We shall make the following assumptions:

1. Total flow entering the off-ramp, $\hat{f}^{in}_{222}$, at any given time is known (from measurements) and is not restricted by the off-ramp supply: $\hat{f}^{in}_{222} < R_{222}$.

2. All the flow coming from the on-ramp (link 111), if such flow exists, is directed toward the GP link 2. In other words, $\beta^c_{111,2} = 1$ and $\beta^c_{111,222} = 0$, $c = 1, \ldots, C$.

3. Demand S^c_i, $i = 1, 111$, $c = 1, \ldots, C$, and supply R_2 are given.

4. Denote the set of destination-based commodities as $\mathcal{D}$. Split ratios β^c_{1j} for $c \in \mathcal{D}$ are known. Split ratios $\beta^c_{1j} = \beta$ for $c \in \overline{\mathcal{D}}$, where β is to be determined.

The first three assumptions here reproduce assumptions 1, 3 and 5 made for the full access HOV/T lane case. Assumption 4 is a reminder that there is a portion of traffic flow that we cannot direct to or away from the off-ramp, but we have to account for it.

Similarly to the full access HOV/T case, define function $\psi(\beta)$:

$$\psi(\beta) = \sum_{c \in \overline{\mathcal{D}}} f^c_{1,222} + \sum_{c \in \mathcal{D}} f^c_{1,222} - \hat{f}^{in}_{222}, \tag{2.7.10}$$

where $f^c_{1,222}$, $c = 1, \ldots, C$ are determined by the node model from step 6 of the simulation model (Section 2.2). The first term of the right-hand sight of (2.7.10) depends on β. As before, $\psi(\beta)$ is a monotonically increasing function. We look for the solution of equation (2.7.9) on the interval $[0, 1]$. This solution exists iff $\psi(0) \leq 0$ and $\psi(1) \geq 0$. The algorithm for finding β is the same as the one presented in the previous section, except that $\underline{b}(0)$ should be initialized to 0, and S_{11} is to be assumed 0.

2.7.8 Summary of the Calibration Process

The model calibration follows the workflow diagram shown in Figure 2.16.

1. We start by assembling the available measurement data. Fundamental diagrams are assumed to be given. Mainline and on-ramp demand is specified per 5-minute periods together with the HOV portion parameter indicating the fraction of the input demand that is HOV. Initially we do not know off-ramp split ratios as they cannot be measured directly. So we use some arbitrary values to represent them and call it "initially guessed off-ramp split ratios". What can be measured instead of off-ramp split ratios, are the flows directed to off-ramps, to which we refer to as *off-ramp demand*. Finally, if we model the HOT lane, we need the readiness to pay coefficients $\alpha_0, \alpha_1, \alpha_2$ for equation (2.4.2), obtained as descibed in Section 2.7.

2. We run the simulation model as described in Section 2.2, where in step 5 the a priori undefined split ratios between traffic in the GP and in the HOV/T lanes (see expressions (2.3.1) and (2.4.1)) will be assigned.

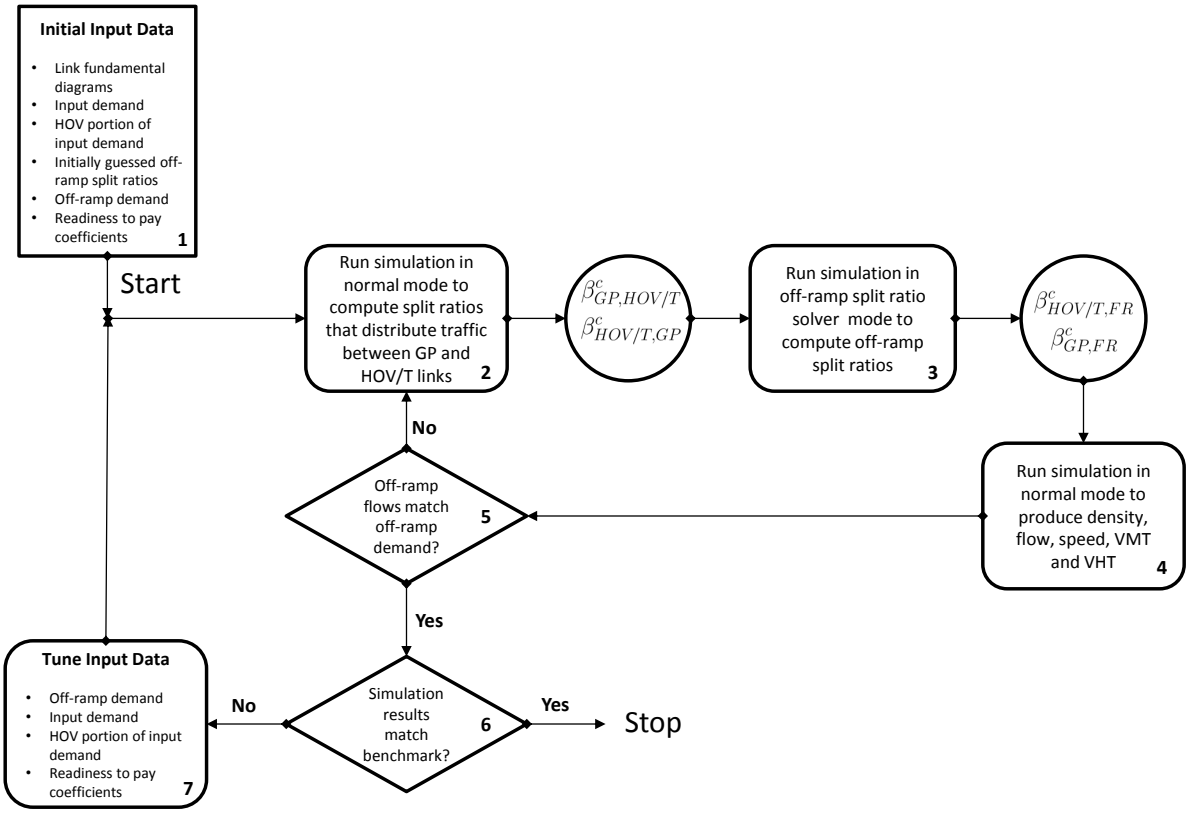

Figure 2.16: Calibration workflow.

3. Using these newly assigned split ratios we run the simulation model again, only this time, instead of using given off-ramp split ratios, we compute them from the given off-ramp demand as described in Sections 2.7.6 and 2.7.7. As a result of this step, we obtain new off-ramp split ratios.

4. Now we run the simulation model as we did originally, in step 2, only this time with new off-ramp split ratios, and record the simulation results — density, flow, speed, as well as performance measures such as vehicle miles traveled (VMT) and vehicle hours traveled (VHT).

5. Check if the resulting off-ramp flows match the off-ramp demand. If yes, proceed to step 6, otherwise, repeat steps 2-5. Usually, it takes the process described in steps 2-5 no more than two iterations to converge.

6. Evaluate the simulation results:

- correctness of bottleneck locations and activation times;
- correctness of flows coming out of bottlenecks;
- correctness of congestion extension at each bottleneck;
- correctness of VMT and VHT.

If the simulation results are satisfactory, stop. Otherwise, proceed to step 7.

7. Tune input data in the order shown in block 7 of Figure 2.16.

Chapter 3

Case Studies

In this chapter we shall present three case studies:

- I-680 North in Contra Costa County — freeway segment with full access HOV lane;
- I-210 East in Los Angeles — freeway segment with limited access HOV lane; and
- I-10 West — freeway segment with limited access HOT lane.

Simulation data presented in this chapter are stored in the corresponding spreadsheets that can be accessed at [3].

3.1 Full Access HOV Lane: I-680 North

We consider a 26.8-mile stretch of I-680 North freeway in Contra Costa County from postmile 30 to postmile 56.8, shown in Figure 3.1, as a test case for the full access HOV lane configuration. This freeway stretch contains two HOV lane segments whose begin and end points are marked on the map. The first HOV segment is 12.3 miles long and will be converted to HOT in spring 2017 [13], and the second HOV segment is 4.5 miles long. There are 26 on-ramps and 24 off-ramps. The HOV

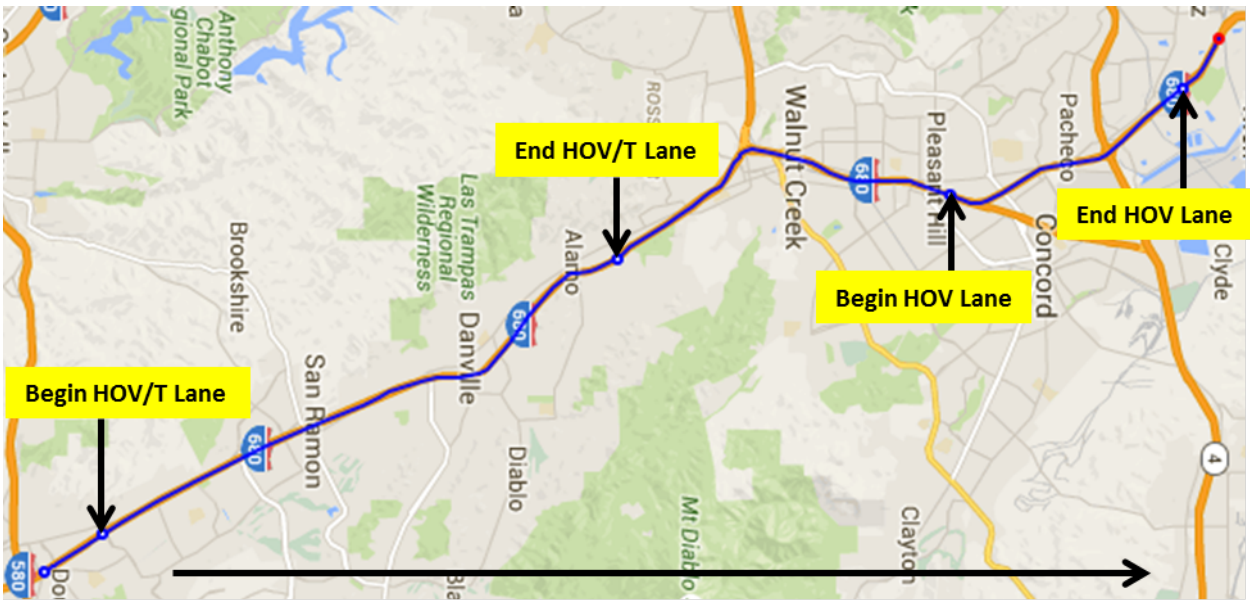

Figure 3.1: Map of I-680 North in Contra Costa County.

lane is active from 5 to 9 am and from 3 to 7 pm. The rest of the time the HOV lane behaves as a GP lane.

To build the model, we used data collected for the I-680 Corridor System Management Plan (CSMP) study [14]. The bottleneck locations as well as their activation times and congestion extension were identified in that study using video monitoring and tachometer vehicle runs. On- and off-ramp flows were given in 5-minute increments. Here we assume that HOV portion of the input demand is 15%. The model was calibrated to a *typical weekday*, as suggested in the I-680 CSMP study. One of the assumptions during the model calibration was that the HOV lane always stays in free flow.

Fundamental diagrams were assigned as follows:

- Capacity of the ordinary GP lane is 1,900 vphl;
- Capacity of the auxiliary GP lane is 900 vphl;
- Capacity of HOV lane is 1,800 vphl while active and 1,900 vphl when it behaves as a GP lane;
- Free flow speed varies between 63 and 70 mph — its measurements came partially from PeMS [5] and partially from tachometer vehicle runs.

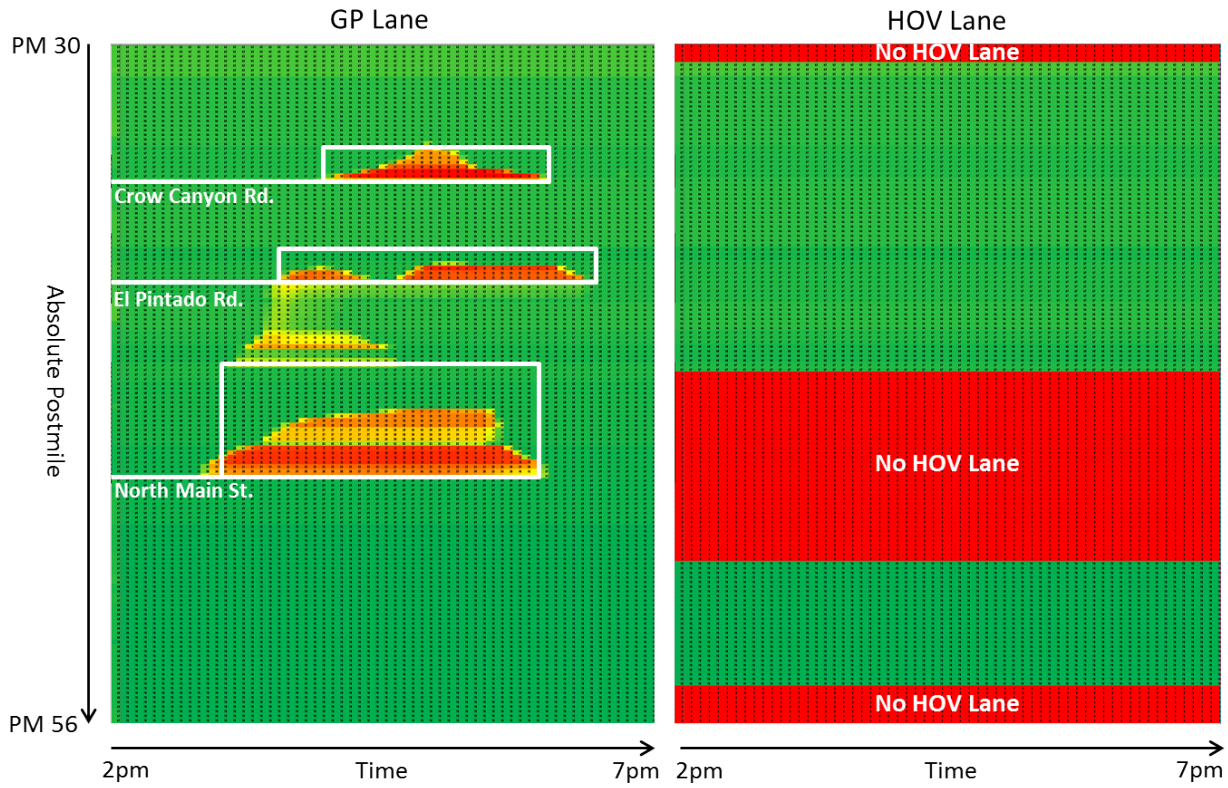

Figure 3.2: I-680 North speed contours for GP and HOV lanes produced by simulation. Speed values are given in miles per hour. White boxes on the GP lane speed contour indicate congested areas as identified by the I-680 CSMP study.

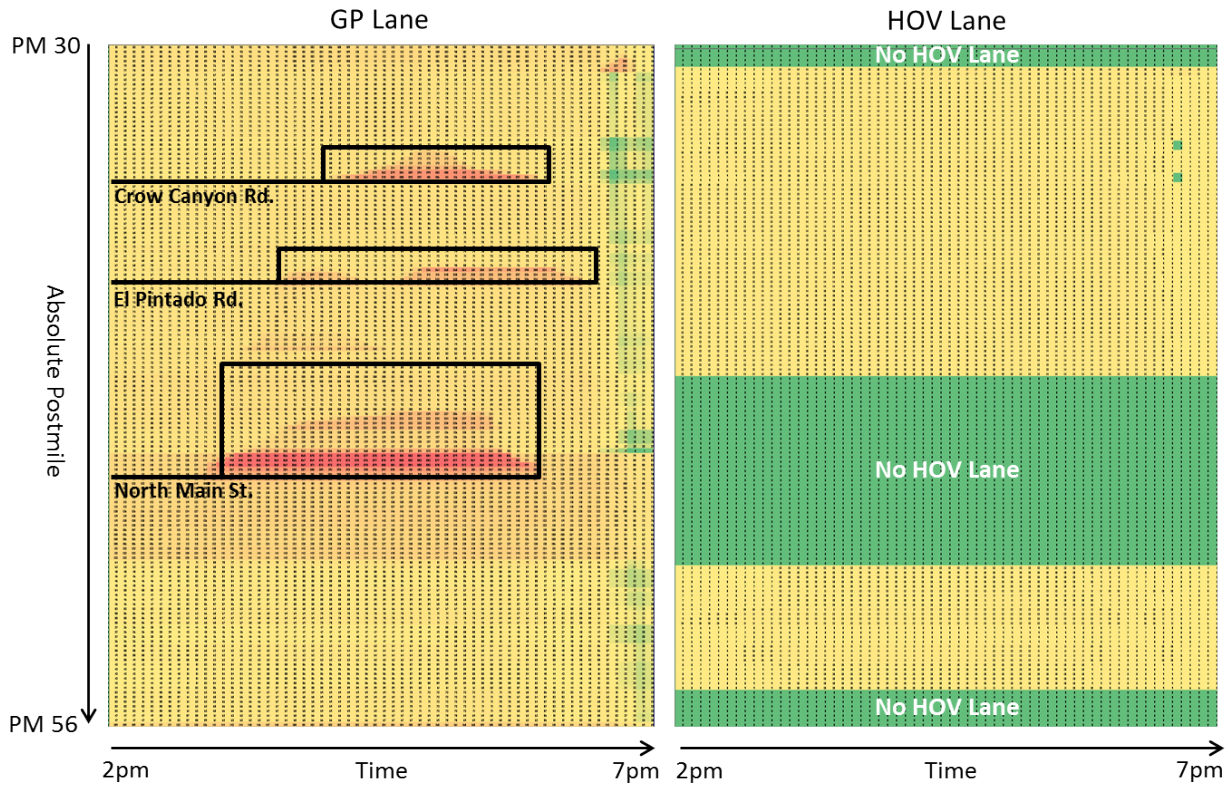

Figure 3.3: I-680 North density contours for GP and HOV lanes produced by simulation. Density values are given in vehicles per mile per lane. Black boxes on the GP lane speed contour indicate congested areas as identified by the I-680 CSMP study.

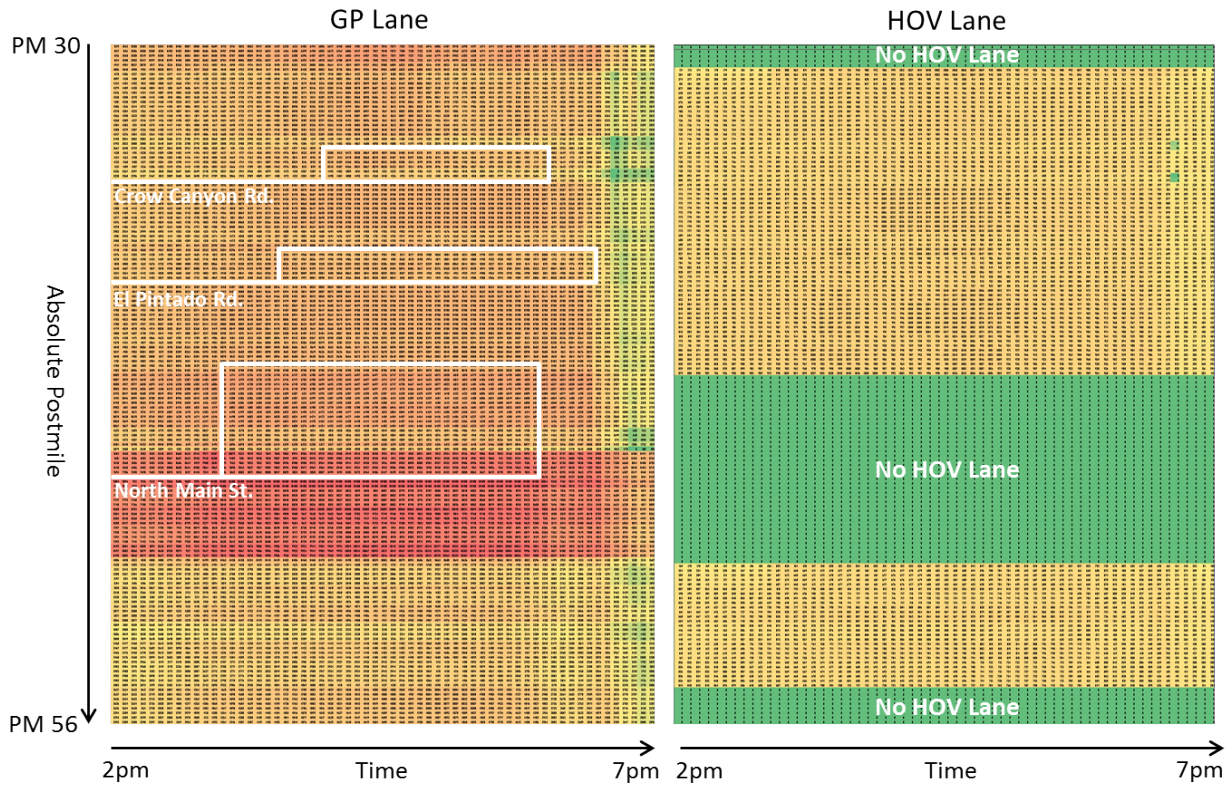

Figure 3.4: I-680 North flow contours for GP and HOV lanes produced by simulation. Flow values are give in vehicles per hour per lane. White boxes on the GP lane speed contour indicate congested areas as identified by the I-680 CSMP study.

Figure 3.5: I-680 North bottlenecks identified in the CSMP study. Source: [14].

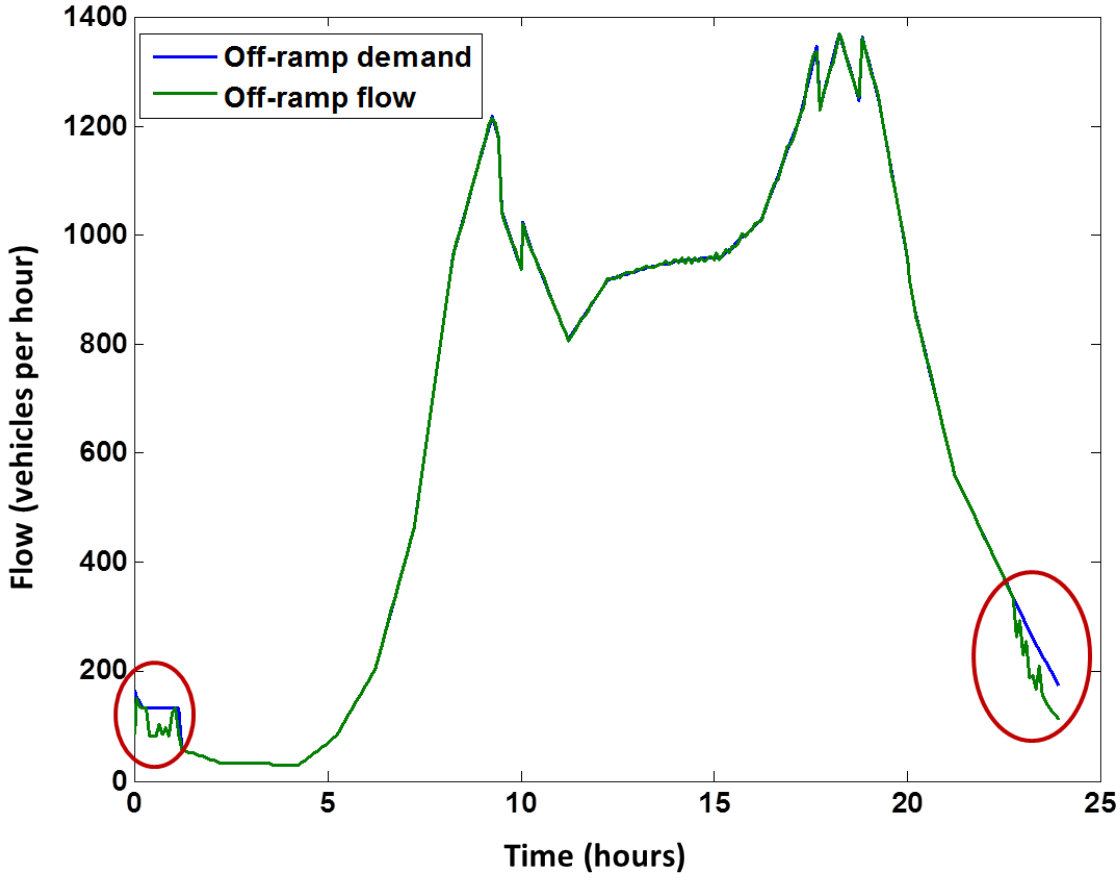

Figure 3.6: Flow at the Crow Canyon Road off-ramp over 24 hours — collected (off-ramp demand) vs. computed by simulation (off-ramp flow).

- Congestion wave speed for each link was taken as 1/5 of the free flow speed.

The modeling results are presented in Figures 3.2, 3.3 and 3.4 showing speed, density and flow contours for the time between 2 and 7 pm in the GP and the HOV lanes respectively.[1] Each of these plots consists of the left, corresponding to the GP lane, and right, corresponding to the HOV lane, parts. In all the plots traffic moves from top to bottom along the "Absolute Postmile" axis, while the horizontal axis represents time. Bottleneck locations and congestion areas identified by the I-680 CSMP study are marked by white and black boxes in GP lane contours. HOV lane does not get congested.

Figure 3.5 shows the snapshot of the three major bottlenecks extracted from the I-680 CSMP

[1]These 5 hours were chosen out of the 24-hour simulation period.

study [14]. Empirical data documented in that study was used as a benchmark for our simulation.

Figure 3.6 shows the example of how well the off-ramp flow computed by the simulation matches the target, referred to as *off-ramp demand*, taken from the off-ramp at Crow Canyon Road. We can see that in the beginning and in the end of the day the computed flow falls below the target (corresponding areas are marked with red circles). Why is this happening? Recall that off-ramp demand is the vehicle count collected at the off-ramp. In the I-680 CSMP study on- and off-ramp counts came mainly from Census tube measurements. Taken on different days, these counts may be inconsistent: fewer vehicles enter the freeway than the number of vehicle that must exit. If the mainline has fewer vehicles than the off-ramp requests, then the off-ramp flow falls below the target. That is the reason why Crow Canyon Road off-ramp is "underfed".

Finally, Table 3.1 summarizes the performance measurements — vehicle miles traveled (VMT), vehicle hours traveled (VHT) and delay in vehicle-hours — computed by simulation versus collected in the course of the I-680 CSMP study. Delay is computed for vehicles with speed below 45 mph.

	Simulation result	Collected data
GP Lane VMT	1,687,618	-
HOV Lane VMT	206,532	-
Total VMT	1,894,150	1,888,885
GP Lane VHT	27,732	-
HOV Lane VHT	3,051	-
Total VHT	30,783	31,008
GP Lane Delay	2,785	-
HOV Lane Delay	6	-
Total Delay	2,791	2,904

Table 3.1: Performance measures for I-680 North.

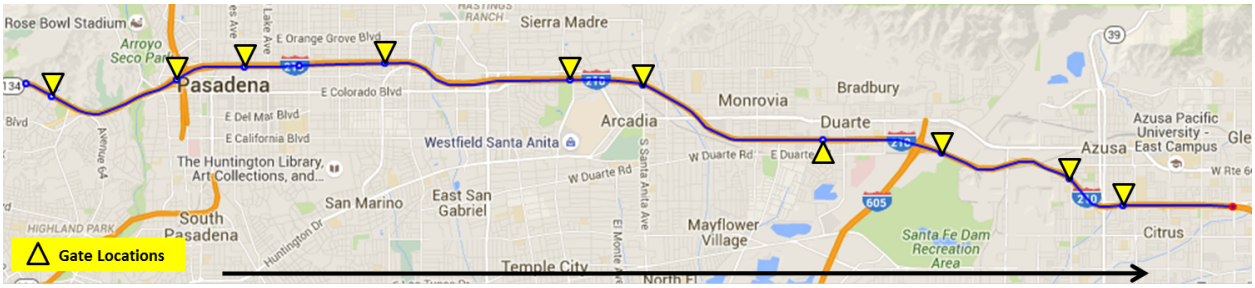

Figure 3.7: Map of SR-134 East/ I-210 East freeway in Los Angeles County.

3.2 Limited Access HOV Lane: I-210 East

We consider a 20.6-mile stretch of SR-134 East/ I-210 East in Los Angeles County shown in Figure 3.7, as a test case for the separated HOV lane configuration. This freeway stretch consists of 3.9 miles of SR-134 East from postmile 9.46 to postmile 13.36 and 16.7 miles of I-210 East from postmile 25 to postmile 41.7. Gate locations, where traffic can switch between the GP and the HOV lanes are marked on the map. The HOV lane is always active. There are 28 on-ramps and 25 off-ramps. The largest number of off-ramps between two gates is 5. Thus, our freeway model has 7 vehicle classes - LOV, HOV and 5 destination-based.

To build the model, we used PeMS data for the corresponding segments of the SR-134 East and I-210 East for Monday, October 13, 2014 [5]. This was one of the days when most vehicle detectors on the GP and the HOV lanes, on-ramps and off-ramps of SR-134 East and I-210 East were intact, and hence the PeMS data are reliable. Fundamental diagrams were calibrated using PeMS data following the methodology [8]. As in the I680 North example, we assume that HOV portion of the input demand is 15% in the off-peak 20% in the peak hours.

The modeling results are presented in Figures 3.8, 3.9 and 3.10 showing speed, density and flow contours for the period between 2 and 7 pm in the GP and the HOV lanes respectively. Each of these plots consists of the left, corresponding to the GP lane, and right, corresponding to the HOV lane, parts. As before, in all the plots traffic moves from top to bottom along the "Absolute Postmile" axis, while the horizontal axis represents time. HOV lane is as congested as the GP lane indicating the fact that the 2+HOV demand is to high for this facility. Dashed white lines on the contour plots indicate HOV gate locations.

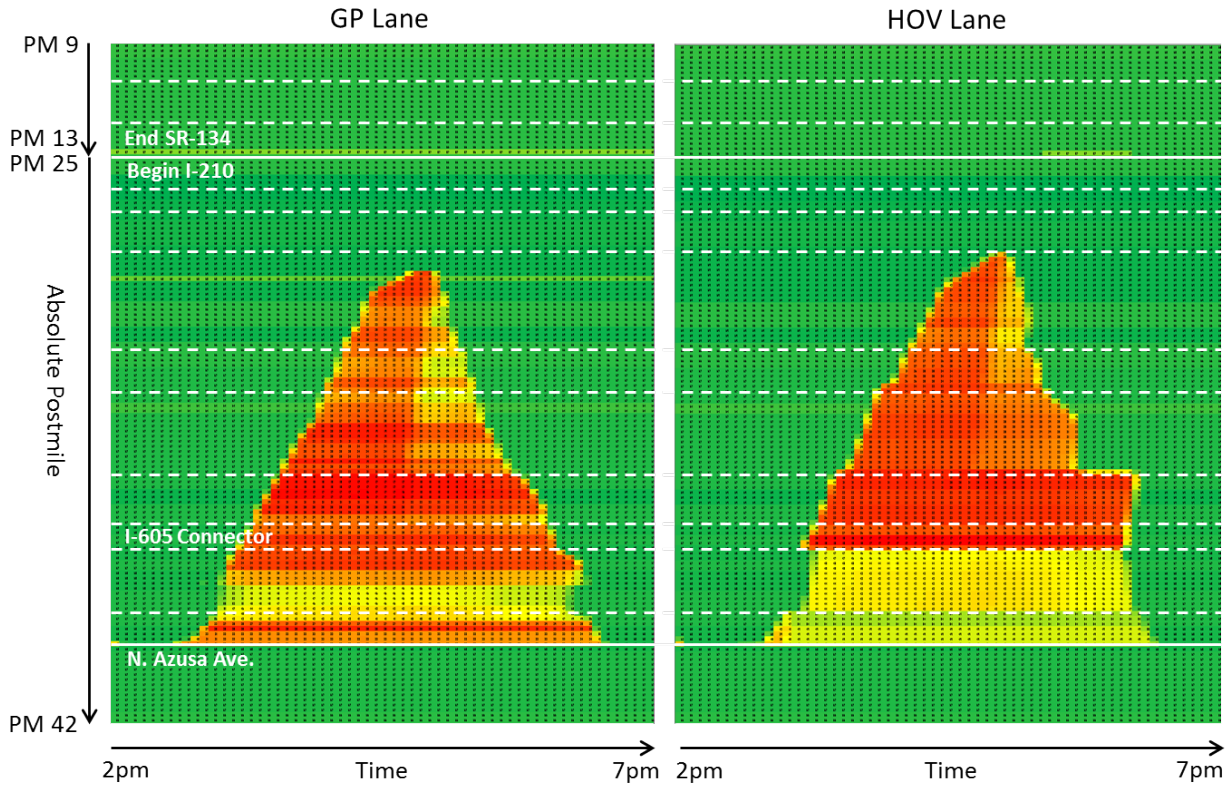

Figure 3.8: SR-134 East/ I-210 East speed contours for GP and HOV lanes produced by simulation.

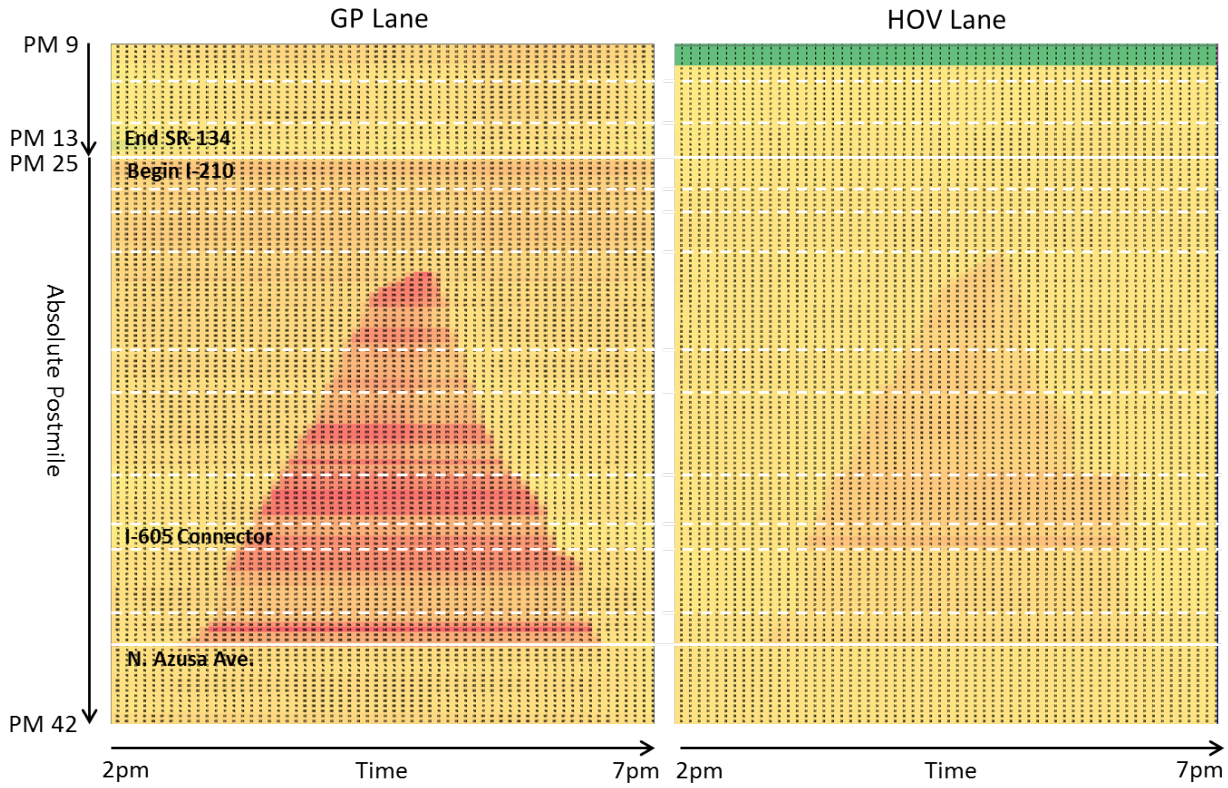

Figure 3.9: SR-134 East/ I-210 East density contours for GP and HOV lanes produced by simulation.

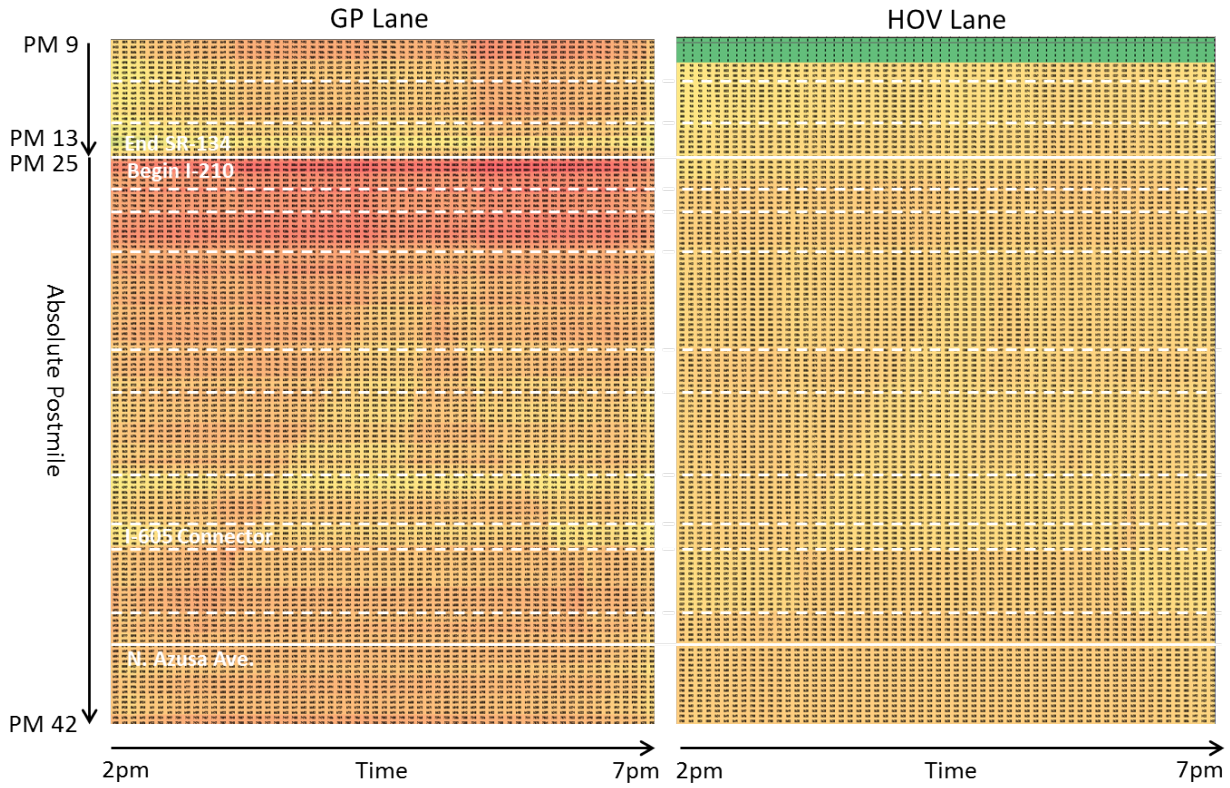

Figure 3.10: SR-134 East/ I-210 East flow contours for GP and HOV lanes produced by simulation.

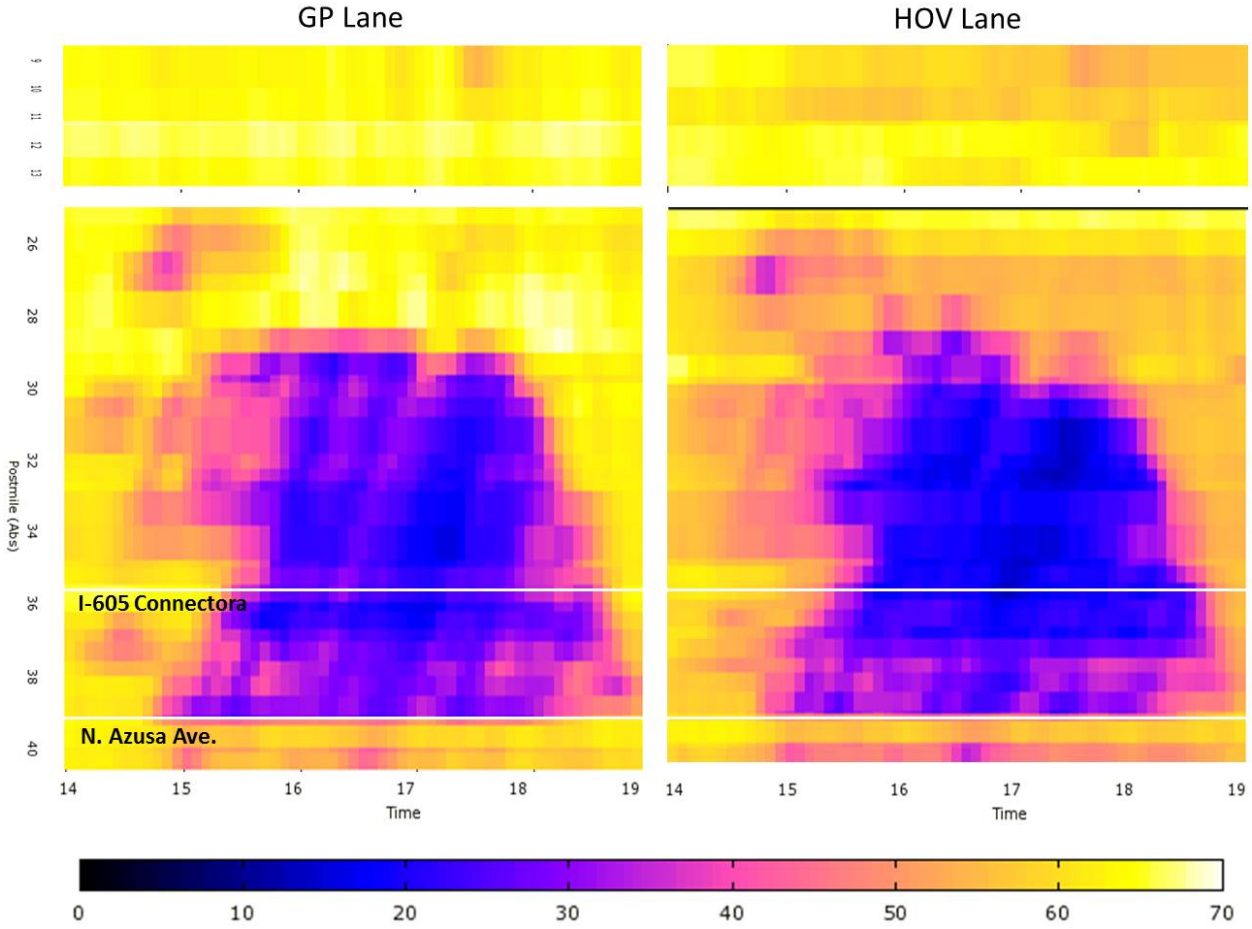

Figure 3.11: SR-134 East/ I-210 East speed contours for GP and HOV lanes obtained from PeMS [5] for Monday, October 13, 2014. Horizontal axis represents time in hours and vertical axis represents absolute postmile.

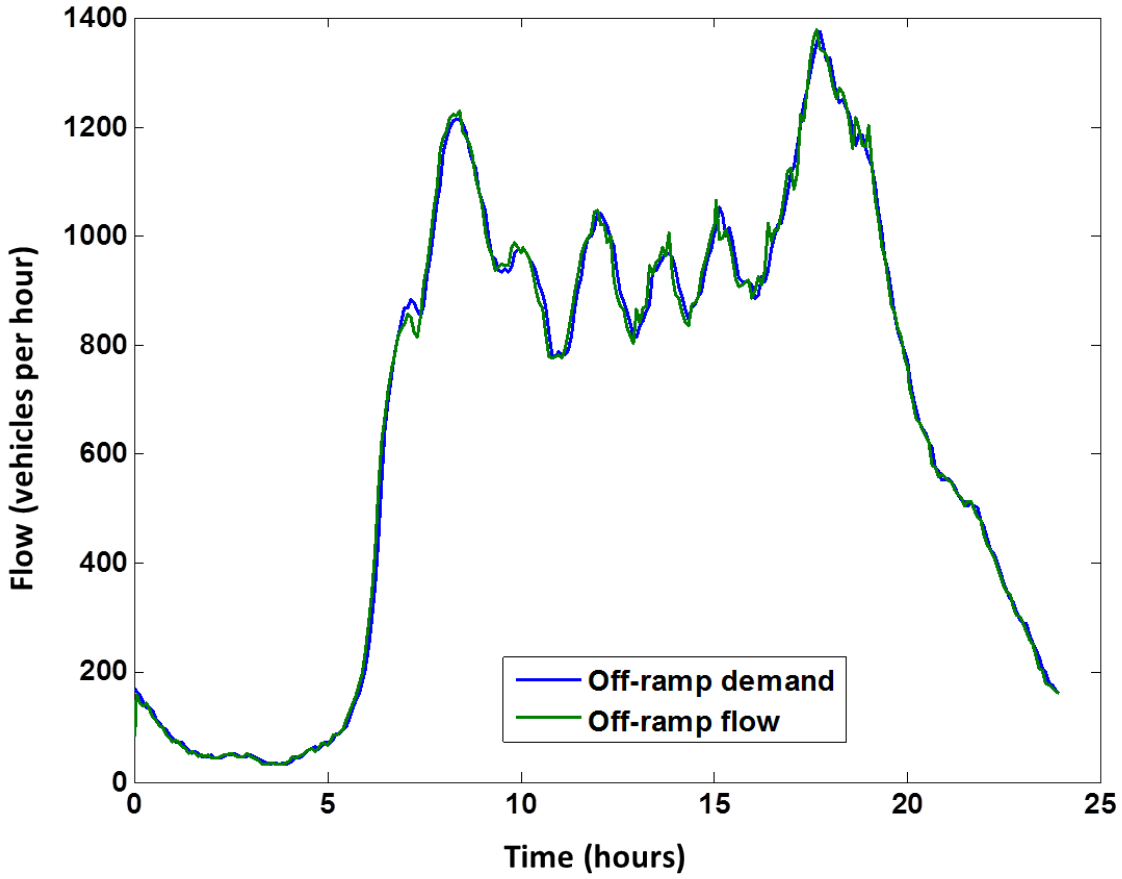

Figure 3.12: Flow at the North Hill Avenue off-ramp over 24 hours — PeMS data (off-ramp demand) vs. computed by simulation (off-ramp flow).

Figure 3.11 shows the PeMS speed contours for the SR-134 East/ I-210 East GP and HOV lanes that were used as a target for our simulation model. In these plots, traffic also travels from top to bottom, with the verticalal axis representing postmiles, while the horizontal axis represents time. The period shown here is between 2 and 7 pm. All four speed contours share the same color scale.

Figure 3.12 shows an example of how well the off-ramp flow computed by the simulation matches the target, referred to as *off-ramp demand*, taken from the off-ramp at North Hill Avenue. The simulated off-ramp flow matches the off-ramp demand not perfectly, but closely enough. So is the case for all the other off-ramps.

Finally, Table 3.2 summarizes the performance measurements — VMT, VHT and delay — computed by simulation versus obtained from PeMS. PeMS data come from both SR-134 East and I-210 East, and VMT, VHT and delay values are computed as sums of the corresponding values from these two freeway sections. Delay values are computed in vehicle-hours for those vehicles travelling slower than 45 mph.

	Simulation result	PeMS data
GP Lane VMT	2,017,322	-
HOV Lane VMT	378,485	-
Total VMT	2,395,807	414,941 + 2,006,457 = 2,421,398
GP Lane VHT	33,533	-
HOV Lane VHT	6,064	-
Total VHT	39,597	6,416 + 36,773 = 43,189
GP Lane Delay	3,078	-
HOV Lane Delay	584	-
Total Delay	3,662	1 + 3,802 = 3,803

Table 3.2: Performance measures for SR-134 East/ I-210 East.

3.3 HOT Lane: I-10 West

To evaluate the proposed model of the HOT controller, we use data from the HOT lane on I-10 West freeway in Los Angeles County [12], a 14-mile freeway with 2 ingress-only, 2 egress-only and 2 ingress/egress gates.[2] In our example we focus on one ingress/egress gate located immediately upstream of South Fremont Avenue exit, shown in Figure 3.13.

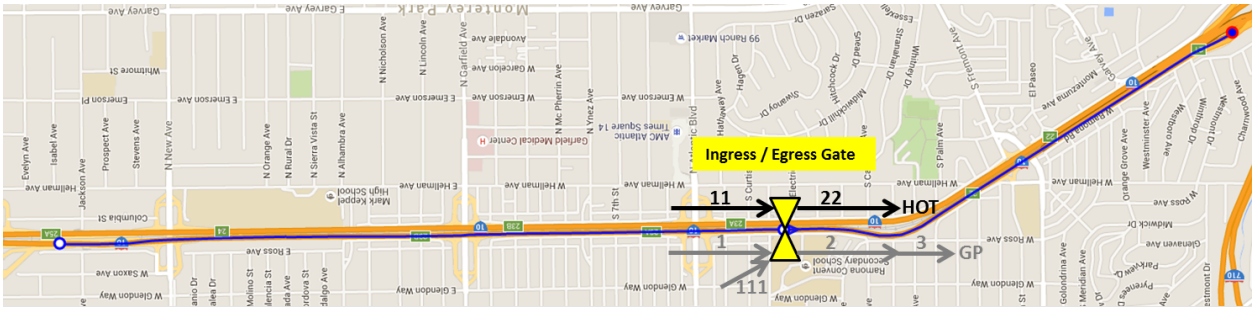

Figure 3.13: Map of the I-10 West freeway section in Los Angeles County near the studied ingress/egress HOT gate.

Here, the GP lane has 4 and the HOT lane has 2 sublanes. The HOT lane is always active, but it has two regimes corresponding to peak hours — from 5 to 9 am and from 4 to 7 pm on weekdays; and to off-peak hours — the rest of the time. During off-peak hours HOVs with two passengers or more can use the HOT lane free of charge, and single-occupancy vehicles (SOVs) can use the HOT lane at the fixed price of 25 cents per mile. During peak hours HOVs with three passengers or more can use the HOT lane free of charge. The others are considered LOVs and to use the HOT lane have to pay the toll that varies between 35 and 140 cents per mile depending on the demand for the HOT lane. During the calibration, our focus is on the HOT controller behavior during peak hours when the HOT lane is dynamically priced between 35 and 140 cents per mile.

We used I-10 West toll data for the year 2014 obtained from LA Metro [12] to calibrate and test the HOT controller. These vehicle counts are collected through FasTrak readers that label each vehicle based on its transponder setting as HOV-3 (3 passengers or more), HOV-2 (2 passengers or more)

[2]Ingress-only gate allows vehicles only to enter the HOT lane. Typically, ingess-only gates are at on-ramps that are directly connected to the HOT lane. Egress-only gate allows vehicles only to exit the HOT lane. Typically, egress-only gates are at off-ramps, to which the HOT lane is connected directly. Ingress/egress gate is a stretch of freeway, where traffic can switch between the GP and HOT lane. In the I-210 East example we dealt with ingress/egress gates.

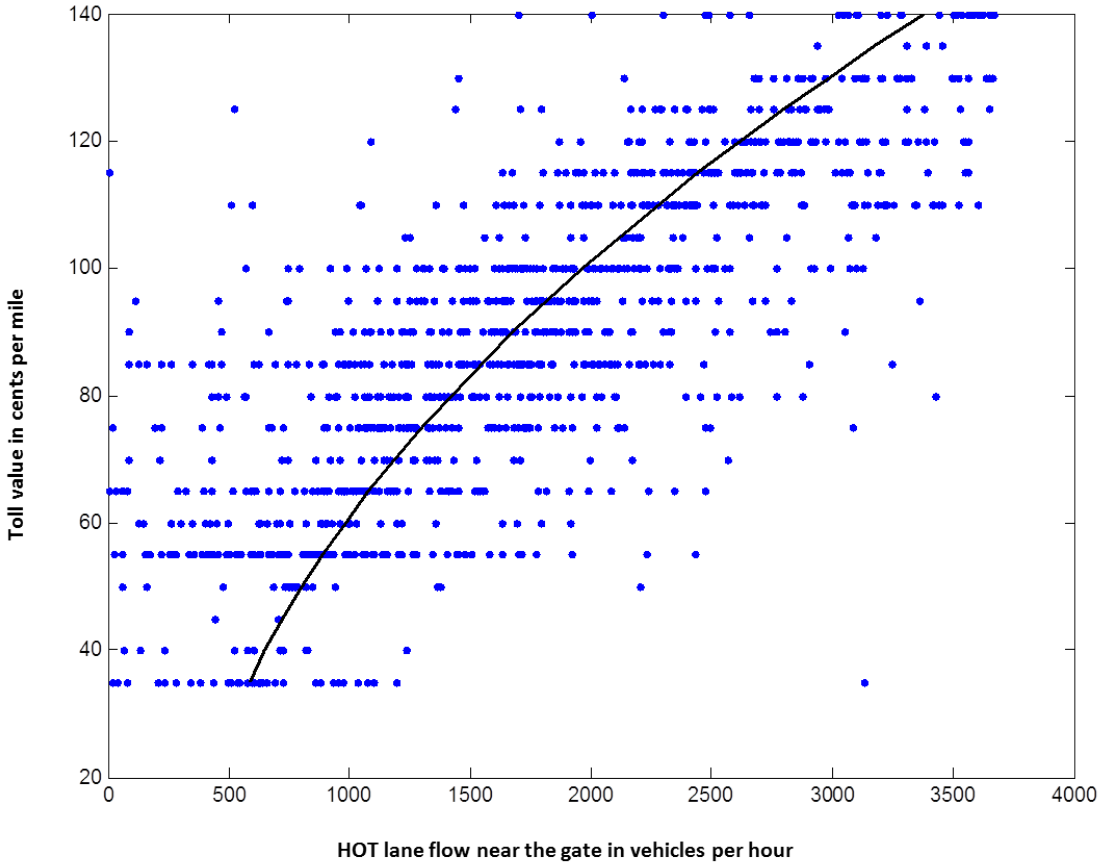

Figure 3.14: Estimation of the toll value based on the flow in the HOT lane.

or SOV. Thus, we know not only the vehicle flow near the FasTrak reader, but how this flow breaks down into HOV and LOV portions.

Remark. Sometimes drivers cheat: a certain number of vehicles with the FasTrak transponder set to HOV-3 are, in fact, SOVs. Our model **does not** identify cheaters. It should be used for assessment of freeway operation provided that there is a given number of self-declared SOVs, HOV-2s and HOV-3s.

We start by building the dependency of the toll value on the vehicle flow in the HOT lane. Figure 3.14 shows this dependency. As we can see, HOT flow varies between 0 and 3,750 vehicles per hour, while the toll value changes in 5-cent increments between 35 and 140 cents per mile. Polynomial curve fitting to the data results in the toll lookup table — Table 3.3. Recall from Section 2.4 that the toll lookup table is the first part of the HOT controller model. as was mentioned there, this

lookup table is typically put together by the operator of the HOT facility. For the purpose of this example, however, we estimated it from the I-10 West toll data.

HOT lane flow in vehicles per hour	Toll value in cents per mile
585	35
651	40
724	45
804	50
890	55
983	60
1,082	65
1,188	70
1,301	75
1,421	80
1,547	85
1,680	90
1,820	95
1,966	100
2,119	105
2,279	110
2,446	115
2,619	120
2,799	125
2,985	130
3,178	135
3,378	140

Table 3.3: Toll lookup table.

The second part of the HOT controller, according to Section 2.4, is the calculation of the portion of LOV traffic ready to pay for using the HOT lane. We obtain the measurement of readiness to pay $\hat{\rho}^t$ from relation (2.7.1) using the I-10 West toll data that allow us to extract the LOV portion of the vehicle counts in the HOT lane for the nominator, and PeMS data for the Vehicle Detector Station (VDS) 716101 [5] for the denominator of the right-hand side of (2.7.1). [3]

Figure 3.15 shows the dependency of $\hat{\rho}^t$ on the difference of vehicle densities in the GP and the HOT lanes obtained from the PeMS VDS 716101 (left), and on the toll value (right). We estimate the portion of LOV traffic ready to pay, ρ, according to the expression (2.4.2), as a function of both the GP-HOT density difference and the toll value. Since we have 4 GP and 2 HOT lanes,

[3] We used data for weekdays of October 2014.

following (2.7.3),

$$\alpha_0 = \ln(2/4) = -0.6931.$$

From the least squares fit (2.7.5)-(2.7.6), we get

$$\alpha_1 = 0.0115, \quad \alpha_2 = -0.0053.$$

Figure 3.16 shows the surface fitting to the data. The resulting readiness to pay ρ as a function of GP-HOT density difference and toll is shown as a 2-dimensional contour in Figure 3.17.

Remark. We should note that for different peak periods and off-peak hours, the readiness to pay function should be estimated on different datasets. For example, in the case of I-10 West, the freeway gets congested only during the morning peak, but in the afternoon peak generally stays in free flow. Nevertheless, the dynamic pricing is still active in the afternoon. Obviously, in periods when freeway is in free flow, the readiness to pay should depend more on the toll value than on the density difference between GP and HOT lanes. In other words, the magnitude of α_2 should be significantly larger than that of α_1. In the HOT controller used for I-10 West simulation described below, we set $\alpha_2 = -0.0626$ for non-peak periods.

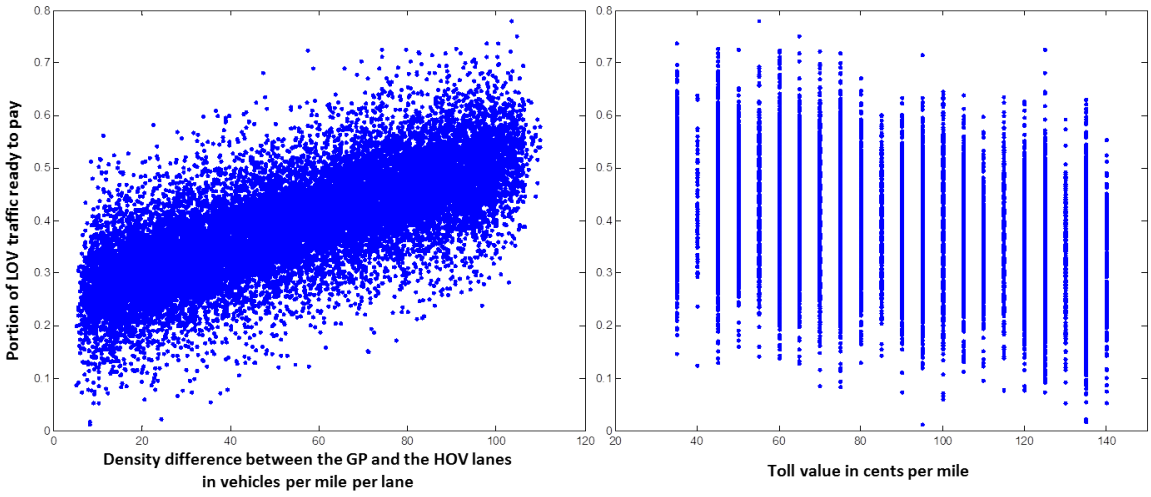

Figure 3.15: Dependency of rediness to pay on difference of traffic density in the GP and the HOT lanes (left); and on the toll value (right).

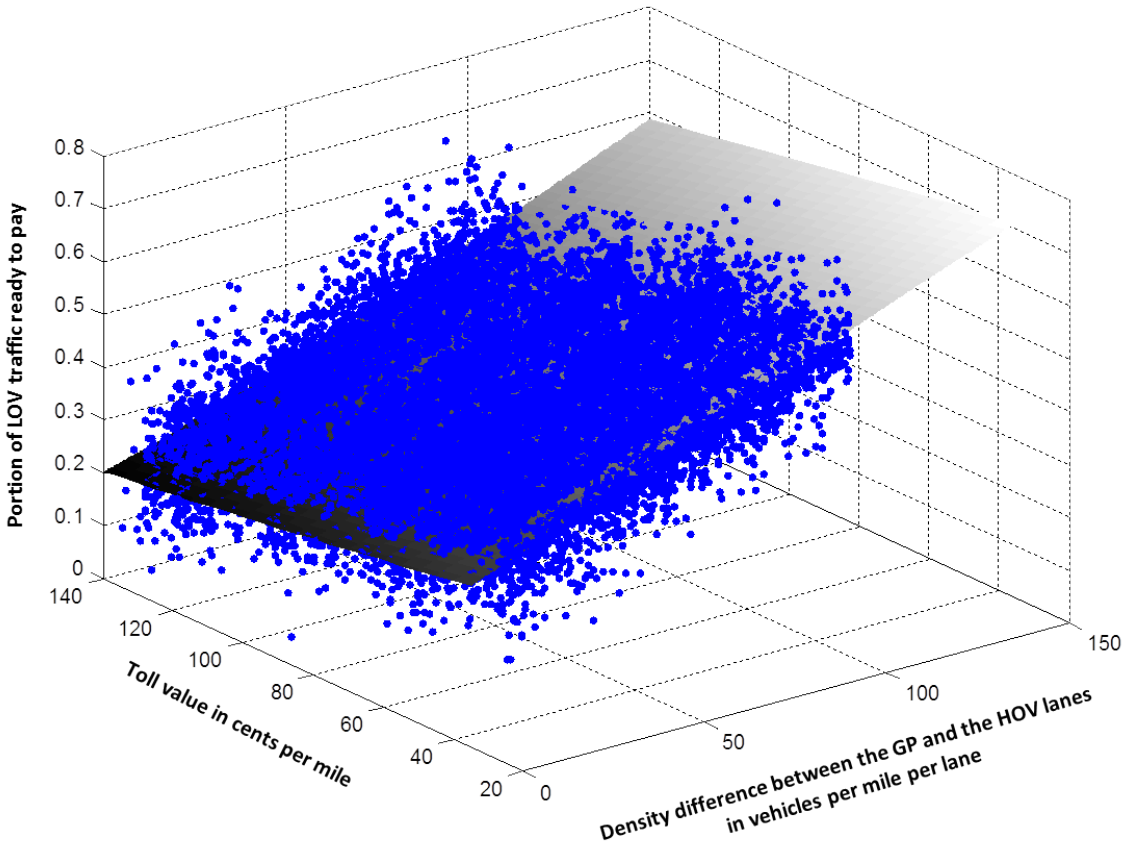

Figure 3.16: Estimation of readiness to pay as a function of density difference between the GP and the HOT lanes and the toll.

Once the HOT controller is calibrated, we test it in three scenarios.

Scenario 1. Consider the road network configuration as shown in Figure 3.13, where link capacities are:

$$F_1 = 8,000 \text{ vph}, \quad F_2 = 8,000 \text{ vph}, \quad F_3 = 1,600 \text{ vph};$$

$$F_{11} = 3,600 \text{ vph}, \quad F_{22} = 3,600 \text{ vph};$$

$$F_{111} = 2,000 \text{ vph}.$$

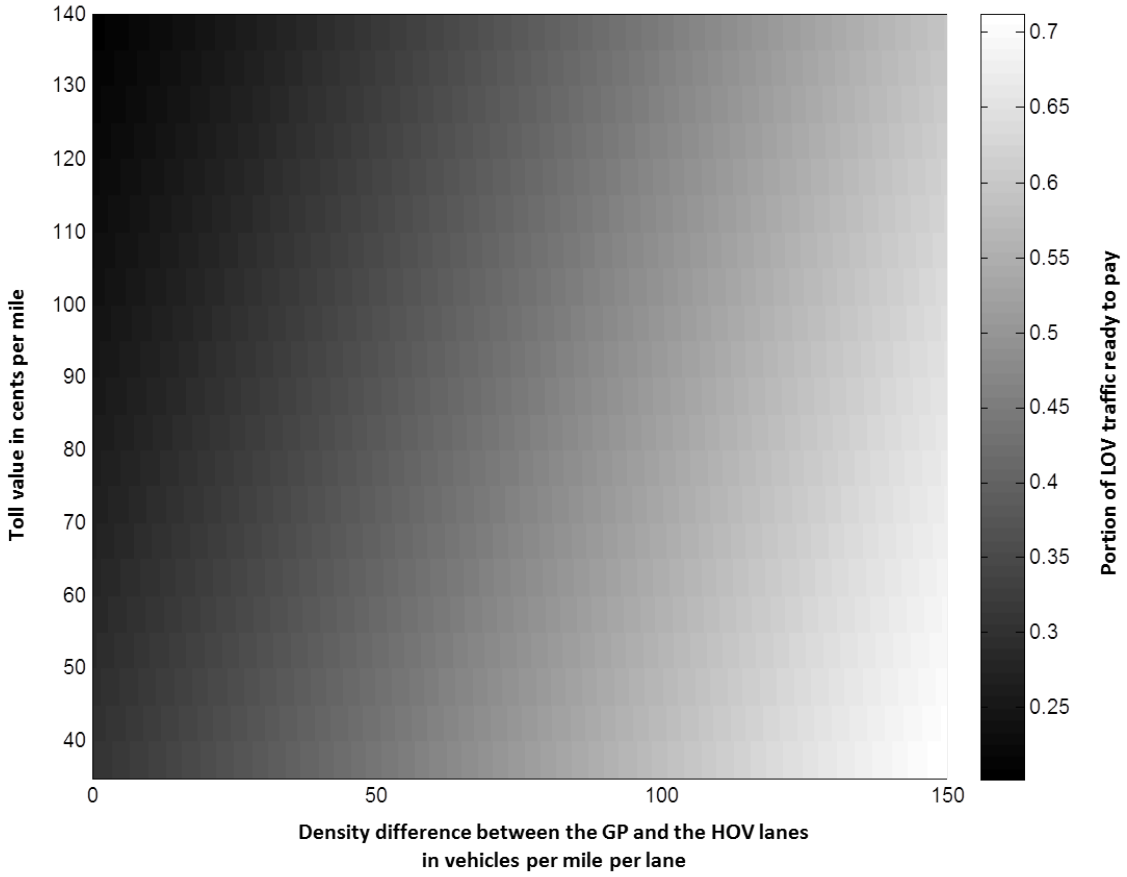

Figure 3.17: Readiness to pay as a function of density difference between the GP and the HOT lanes and the toll.

Input demand for links 1 and 11 is constant:

$$
\begin{aligned}
&d_1^1 = 6,700 \text{ vph}, \quad d_1^2 = 0 \text{ vph}, \quad d_1^3 = 0 \text{ vph};\\
&d_{11}^1 = 0 \text{ vph}, \quad d_{11}^2 = 385 \text{ vph}, \quad d_{11}^3 = 0;\\
&d_{111}^1 = 85 \text{ vph}, \quad d_{111}^2 = 15 \text{ vph}, \quad d_{111}^3 = 0 \text{ vph}.
\end{aligned}
$$

As we can see, GP link 3 with its low capacity creates a bottleneck for traffic that stays in the GP lane.

Figure 3.18 presents the results of the simulation: LOV and HOV input demand (top-left); flows entering the GP link 2 and the HOT link 22 (bottom-left); toll value (top-right); and the portion of LOV traffic ready to pay the corresponding toll. The system reaches the equilibrium at 80 cents

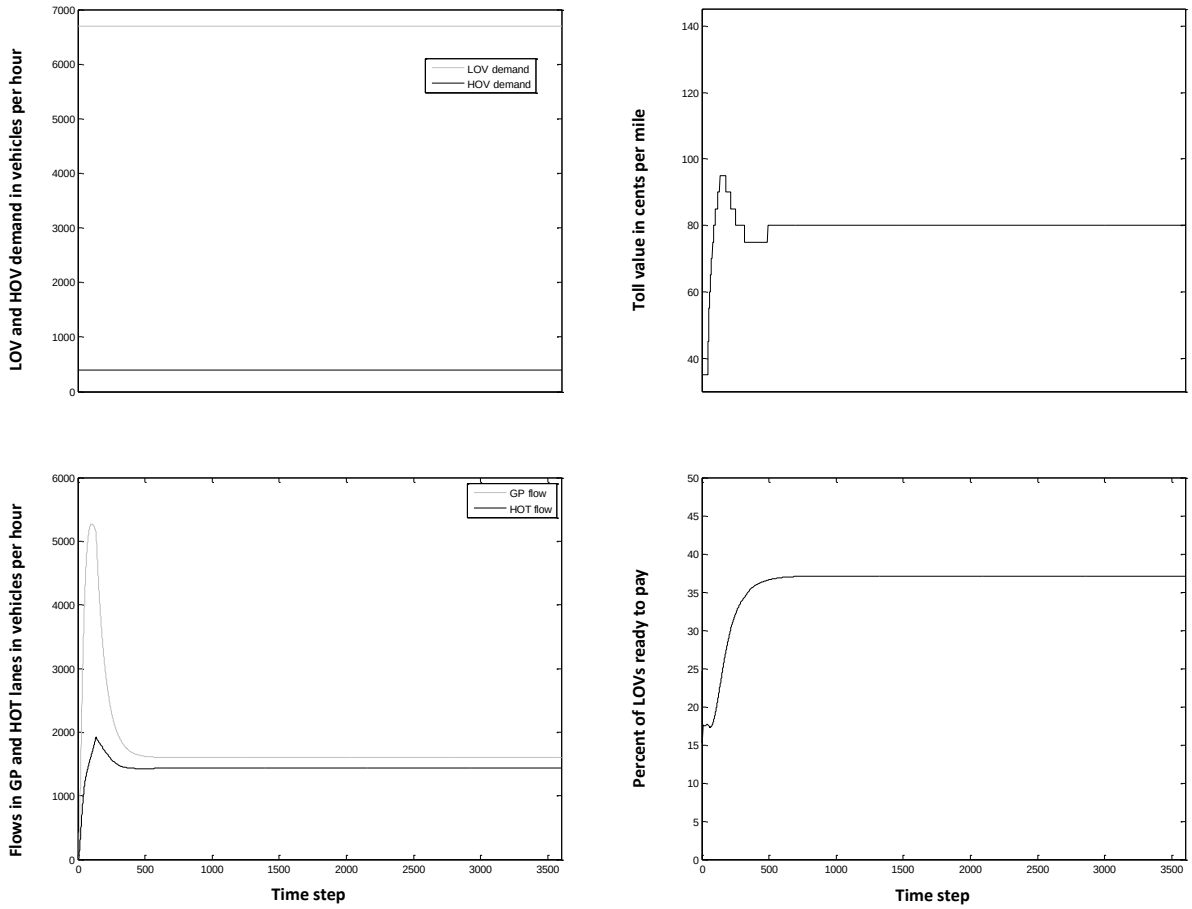

Figure 3.18: Scenario 1 — constant LOV and HOV demand.

per mile with 37% of LOVs ready to pay.

Scenario 2. This scenario differs from the scenario 1 only in the HOV demand coming into the HOT lane:

$$d_{11}^2 = 2,585 \text{ vph.}$$

As shown in Figure 3.19, more vehicles enter now the HOT link 22 (bottom-left); the toll value goes up accordingly, to 135 cents per mile; and the readiness to pay drops to 27%.

Scenario 3. In this scenario, we set capacity of the GP link 3:

$$F_3 = 7,600 \text{ vph.}$$

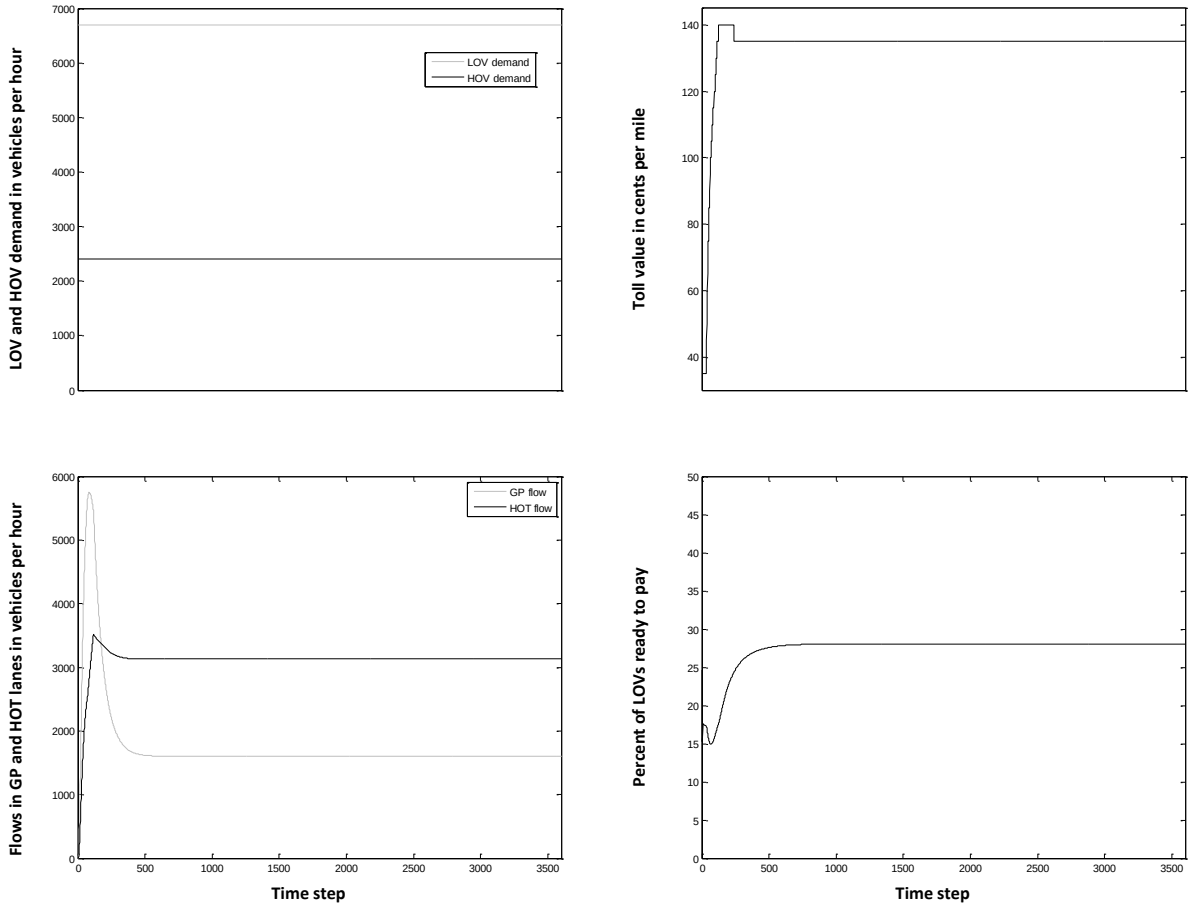

Figure 3.19: Scenario 2 — the same as scenario 1, but has higher HOV demand.

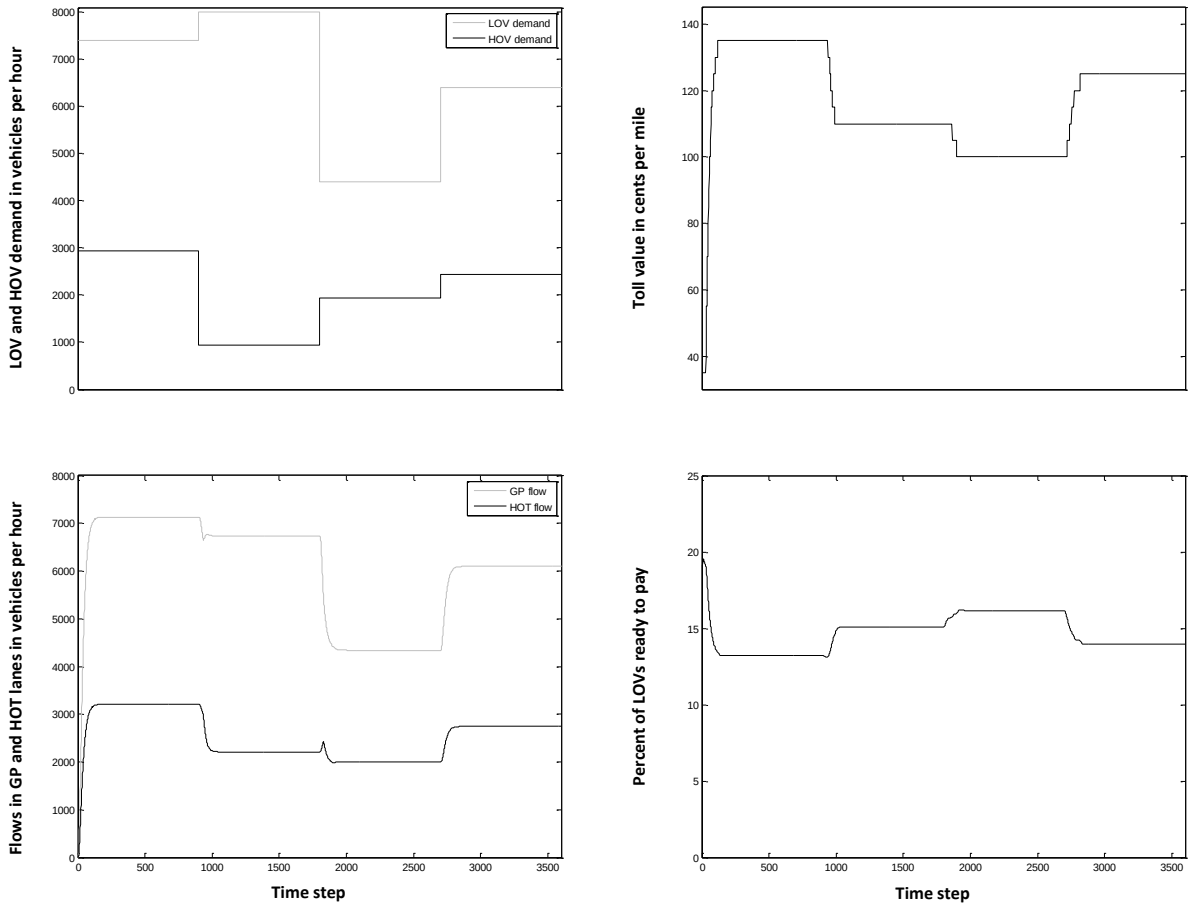

Figure 3.20: Scenario 3 — varying LOV and HOV demand.

The simulation is divided into 4 time periods. The LOV and the HOV demand in links 1 and 11 changes from period to period as specified in Table 3.4.

	Time period 1	Time period 2	Time period 3	Time period 4
d_1^1 (vph)	7,000	7,600	4,000	6,000
d_{11}^2 (vph)	2,940	940	1,940	2,440

Table 3.4: Varying demand.

On-ramp demand is constant:

$$d_{111}^1 = 340 \text{ vph}, \quad d_{111}^2 = 60 \text{ vph}.$$

The results of the simulation are shown in Figure 3.20.

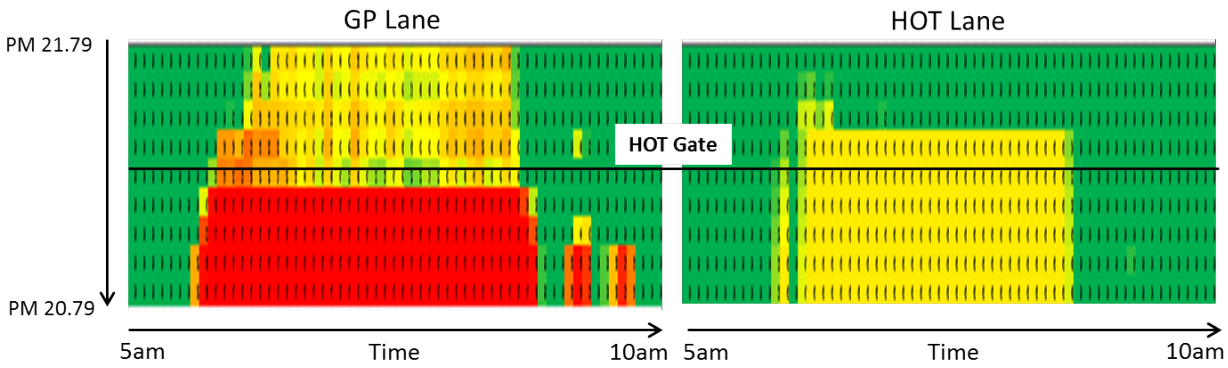

Figure 3.21: I-10 West speed contours for GP and HOT lanes produced by simulation.

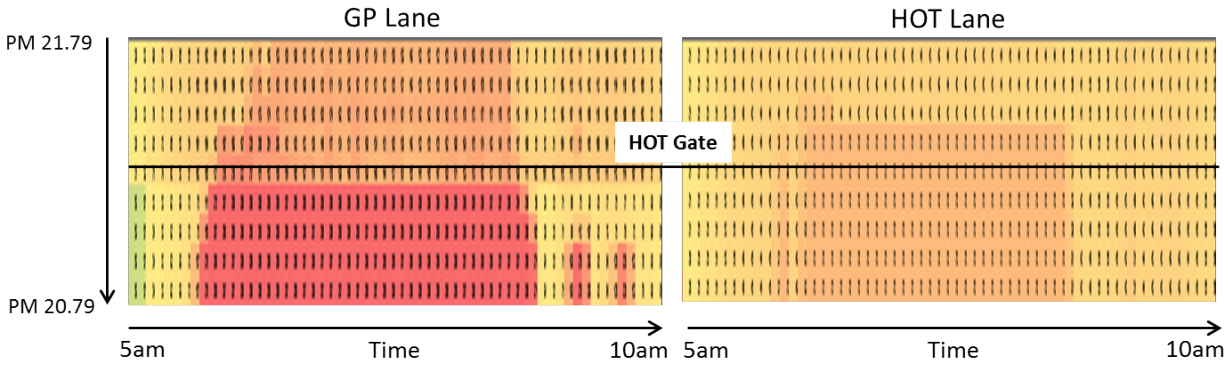

Figure 3.22: I-10 West density contours for GP and HOT lanes produced by simulation.

Now we consider a 1-mile stretch of I-10 West in Los Angeles County shown in Figure 3.13, as a test case for the HOT lane configuration with limited access. This freeway stretchs from postmile v21.79 to postmile 20.79 Gate location, where traffic can switch between the GP and the HOT lanes is marked on the map. The HOT lane is always active. There are 2 on-ramps and 2 off-ramps. The largest number of off-ramps between two gates is 1. Thus, our freeway model has 7 vehicle classes - LOV, HOV, LOV ready to pay and 1 destination-based.

To build the model, we used PeMS data for the corresponding segment of I-10 West for Tuesday, October 14, 2014 [5]. This was one of the days when most vehicle detectors on the GP and the HOT lanes, on-ramps and off-ramps of I-10 West were intact, and hence the PeMS data are reliable. Fundamental diagram parameters were assigned using the default guideline discussed in Section 2.7.1. We assume the HOV portion[4] of the input demand is 20% in the off-peak 25% in the peak hours.

[4]When we discuss HOV traffic on the weekday in the context of I-10, we mean HOV 3+. HOVs 2+ as well as SOVs are considered low occupancy.

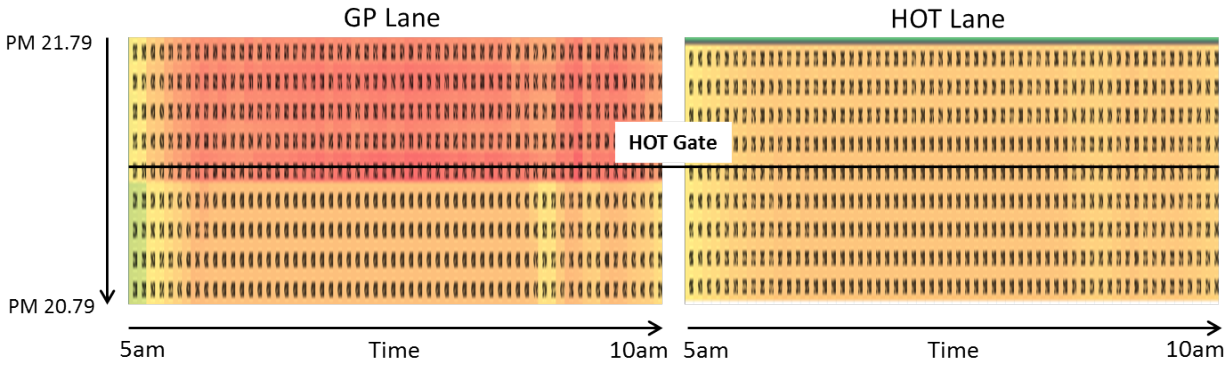

Figure 3.23: I-10 West flow contours for GP and HOT lanes produced by simulation.

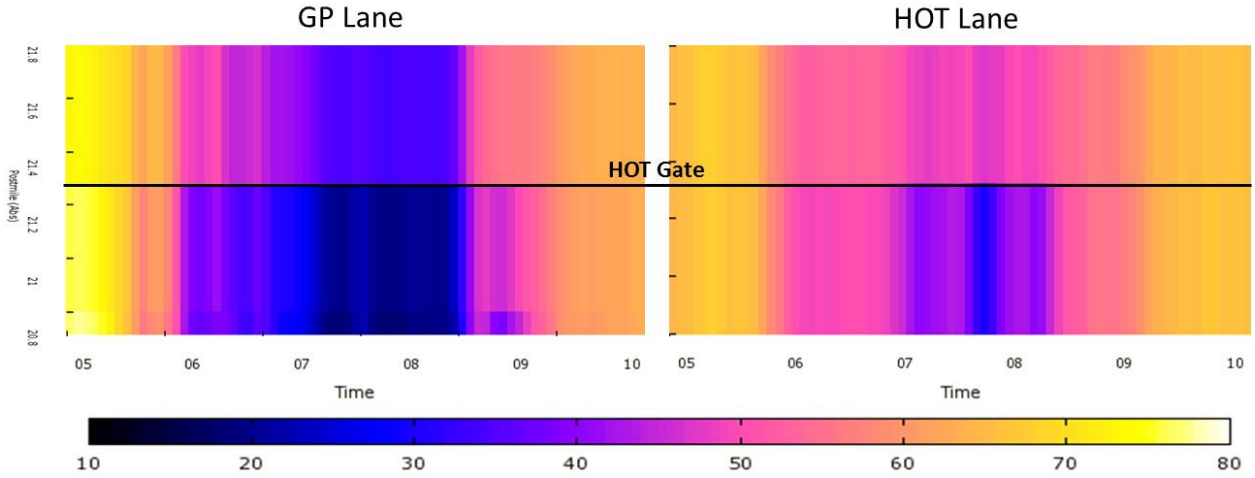

Figure 3.24: I-10 West speed contours for GP and HOT lanes obtained from PeMS [5] for Tuesday, October 14, 2014. Horizontal axis represents time in hours and vertical axis represents absolute postmile.

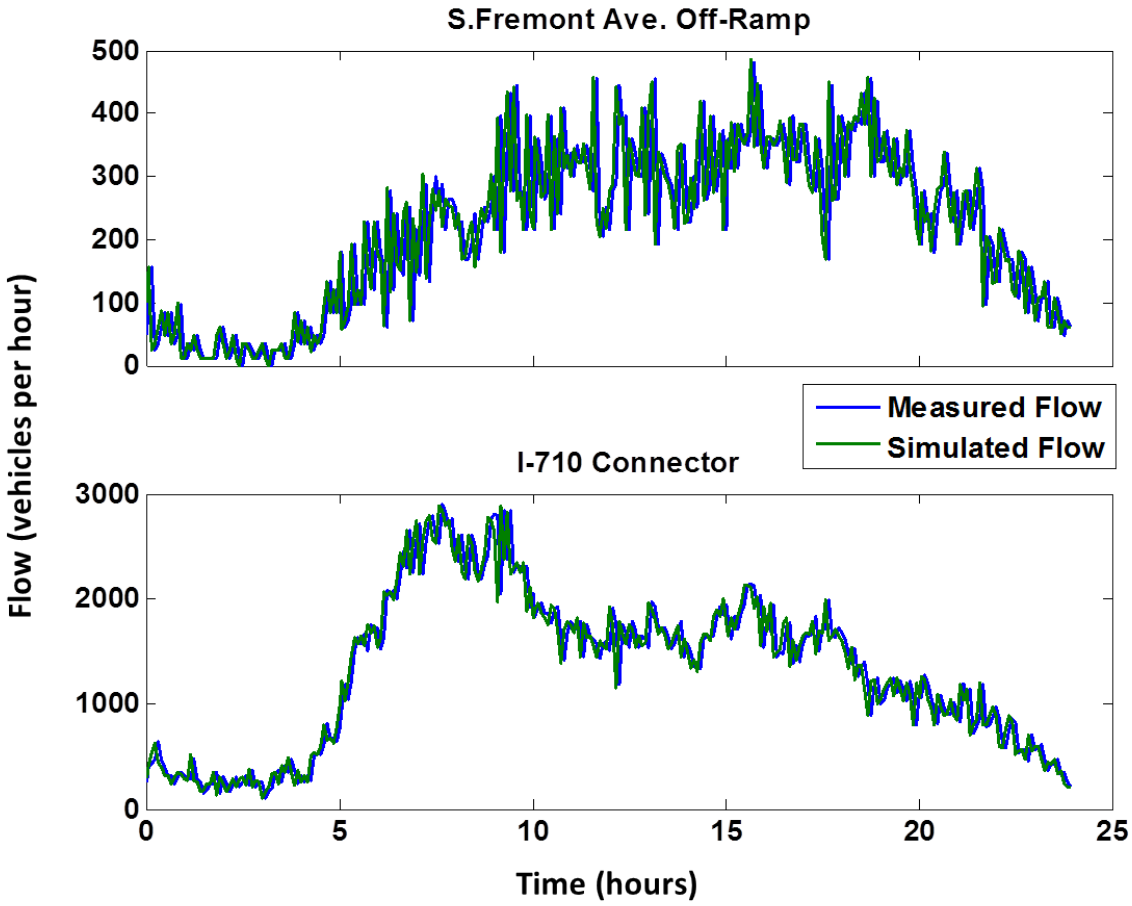

Figure 3.25: 5-minute flows at the I-10 West off-ramps over 24 hours — PeMS data (measured flow) vs. computed by simulation.

The reason for so high numbers is that empirical evidence suggests that there are a lot of violators — SOVs declaring themselves as HOVs 3+ — at the I10 HOT lane during peak hours.

The modeling results are presented in Figures 3.21, 3.22 and 3.23 showing speed, density and flow contours for the period between 5 and 10 am in the GP and the HOT lanes respectively. Each of these plots consists of the left, corresponding to the GP lane, and right, corresponding to the HOT lane, parts. As before, in all the plots traffic moves from top to bottom along the "Absolute Postmile" axis, while the horizontal axis represents time. Black lines o the contour plots indicate HOT gate location.

Figure 3.24 shows the PeMS speed contours for the I-10 West GP and HOT lanes that were used as a target for our simulation model. In these plots, traffic also travels from top to bottom, with the verticalal axis representing postmiles, while the horizontal axis represents time. The period shown here is between 5 and 10 am. Both speed contours share the same color scale.

Figure 3.25 shows how well the off-ramp flows computed by the simulation match the measurements taken at the South Fremont Ave. and I-710 off-ramps.

Table 3.5 summarizes the performance measurements for the modeled segment of I-10 West — VMT, VHT and delay — computed by simulation versus obtained from PeMS. Delay values are computed in vehicle-hours for those vehicles travelling slower than 45 mph.

	Simulation result	PeMS data
GP Lane VMT	76,287	-
HOT Lane VMT	28,466	-
Total VMT	104,753	115,076
GP Lane VHT	1,484	-
HOT Lane VHT	459	-
Total VHT	1,943	2,252
GP Lane Delay	280	-
HOT Lane Delay	29	-
Total Delay	309	326

Table 3.5: Performance measures for I-10 West.

Figure 3.26 shows plots of how toll per mile was changing during the 24 hours of simulated time (top) and how the percent of LOVs ready to pay was changing during the same period (bottom).

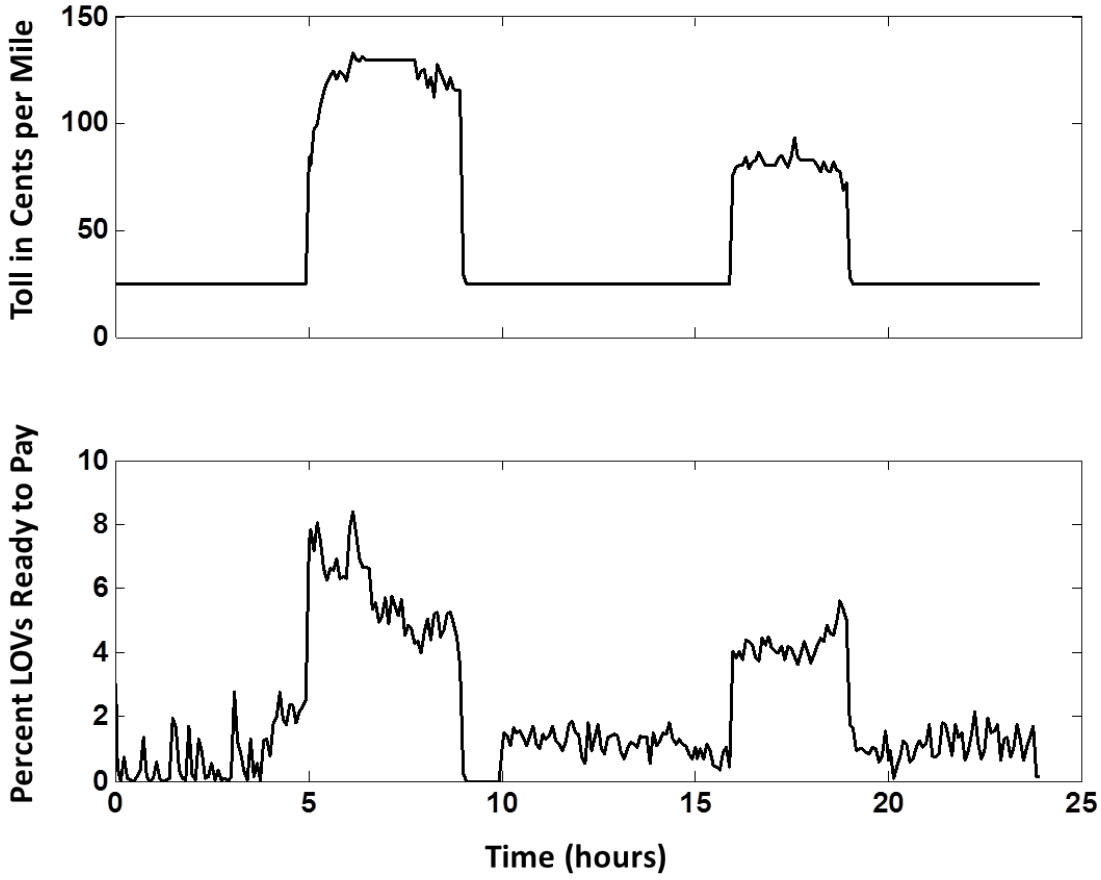

Figure 3.26: Change in toll value (top) and the percent of LOVs ready to pay (bottom) averaged over 5-minute intervals.

These data are averaged over 288 5-minute periods and reported in the *HOT Pricing* and *HOT Ready to Pay* sheets of the spreadsheet, whose snapshots are presented in Figure 3.27.

Toll per Mile Averaged over 5-minute Intervals

	A	B	C	D	E	F	G	H	I	J	BQ	BR	BS	BT	BU	BV	BW	BX	BY	BZ	CA	CB	CC	CD	C
1	GP Link ID	HOV/T Link ID	Postmile	Length (miles)	Detector	Ramp ID	Layout	Name	Comments	0:00	4:55	5:00	5:05	5:10	5:15	5:20	5:25	5:30	5:35	5:40	5:45	5:50	5:55	6:00	6:
2	2	0	21.79	0.100	716091/762486	0	IIIIII			0	0	0	0	0	0	0	0	0	0	0	0	0	0	0	
3	3	1003	21.69	0.100	0	0	\IIIIHH			0	0	0	0	0	0	0	0	0	0	0	0	0	0	0	
4	4	1004	21.59	0.100	0	2003	IIIIHH	OR South Atlantic Blvd	716094	0	0	0	0	0	0	0	0	0	0	0	0	0	0	0	
5	5	1005	21.49	0.100	0	3005	/IIIIHH	FR South Fremont Ave	717072, HOT Gate	25	25	84	80.5	97.25	99.667	108.58	114.33	119.17	121.83	124.67	120.83	124.58	122.83	120.25	12
6	6	1006	21.39	0.100	0	0	\IIIIHH			0	0	0	0	0	0	0	0	0	0	0	0	0	0	0	
7	7	1007	21.29	0.100	0	2006	IIIIHH	OR South Fremont Ave	716089	0	0	0	0	0	0	0	0	0	0	0	0	0	0	0	
8	8	1008	21.19	0.100	0	3008	/IIIIHH	I-710 FR	774578/774579	0	0	0	0	0	0	0	0	0	0	0	0	0	0	0	
9	9	1009	21.09	0.100	0	0	IIIIH			0	0	0	0	0	0	0	0	0	0	0	0	0	0	0	
10	10	1010	20.99	0.100	0	0	IIIIH			0	0	0	0	0	0	0	0	0	0	0	0	0	0	0	
11	11	1011	20.89	0.100	0	0	IIIIH			0	0	0	0	0	0	0	0	0	0	0	0	0	0	0	

Portion of LOV Traffic Ready to Pay

	A	B	C	D	E	F	G	H	I	J	BQ	BR	BS	BT	BU	BV	BW	BX	BY	BZ	CA	CB	CC	CD	C
1	GP Link ID	HOV/T Link ID	Postmile	Length (miles)	Detector	Ramp ID	Layout	Name	Comments	0:00	4:55	5:00	5:05	5:10	5:15	5:20	5:25	5:30	5:35	5:40	5:45	5:50	5:55	6:00	6:
2	2	0	21.79	0.100	716091/762486	0	IIIIII			0	0	0	0	0	0	0	0	0	0	0	0	0	0	0	
3	3	1003	21.69	0.100	0	0	\IIIIHH			0	0	0	0	0	0	0	0	0	0	0	0	0	0	0	
4	4	1004	21.59	0.100	0	2003	IIIIHH	OR South Atlantic Blvd	716094	0	0	0	0	0	0	0	0	0	0	0	0	0	0	0	
5	5	1005	21.49	0.100	0	3005	/IIIIHH	FR South Fremont Ave	717072, HOT Gate	0.0303	0.025	0.0744	0.0784	0.0719	0.0804	0.075	0.0663	0.0626	0.0661	0.066	0.0635	0.0634	0.0638	0.0632	0.
6	6	1006	21.39	0.100	0	0	\IIIIHH			0	0	0	0	0	0	0	0	0	0	0	0	0	0	0	
7	7	1007	21.29	0.100	0	2006	IIIIHH	OR South Fremont Ave	716089	0	0	0	0	0	0	0	0	0	0	0	0	0	0	0	
8	8	1008	21.19	0.100	0	3008	/IIIIHH	I-710 FR	774578/774579	0	0	0	0	0	0	0	0	0	0	0	0	0	0	0	
9	9	1009	21.09	0.100	0	0	IIIIH			0	0	0	0	0	0	0	0	0	0	0	0	0	0	0	
10	10	1010	20.99	0.100	0	0	IIIIH			0	0	0	0	0	0	0	0	0	0	0	0	0	0	0	
11	11	1011	20.89	0.100	0	0	IIIIH			0	0	0	0	0	0	0	0	0	0	0	0	0	0	0	

Figure 3.27: Snap shots of HOT Pricing (top) and HOT Ready to Pay (bottom) sheets.

Chapter 4

Conclusion

In the course of this project a simulation framework ffor freeways with managed lanes [4] was developed around the Berkeley Advanced Traffic Simulator (BeATS) [1]. It was tested with freeway segments of I-680 North (full access HOV lane), I-210 East (limited access HOV lane) and I-10 West (limited access HOT lane). As test examples show, the smulation can adquately reproduce traffic behavior in the presence of multiple vehicle classes and managed lane facilities. Model calibration guidelines are provided.

This project is an important step in the development of the open source software package for operations planning in multimodal transportation networks. The implemented framework enables the following analyses:

- estimate impact of different freeway traffic modes on system performance;
- optimize ramp metering plans;
- determine the cause of congestion — excessive demand or poor operational strategy.

Historical toll data, together with vehicle counts, enable the estimation of willingness to pay for LOVs, making HOT revenue analysis possible:

- given a traffic pattern, estimate HOT revenue projections;

- optimize dynamic toll strategy.

The developed simulation framework has some limitations that require further research to be overcome. Some of these limitations are just the absence of certain nice-to-have features, such as:

- connection to the 4-step travel demand model, which would allow seemless development of future year projections;
- inclusion of arterial signals adjacent to freeway on- and off-ramps.

More important is the ability to assess impact of violators on HOV/T facility's operational and fiscal performance. The implemented HOT controller has no knowledge about cheaters, SOVs that declare themselves HOVs to avoid the toll, and uses data collected from FasTrak transponders as is. The other type of violations, specific to limited access facilities, is the crossing between GP and HOV/T lanes through the barrier (solid white line). Empirical data suggest that such violations are common, and it is important to quantify their impact. It is possible to extend the existing simulation model to include violator vehicle class with its behavior model.

The most significant limitation of the current simulation framework is that currently it is built in MATLAB. An incremental step is required to make it usable for Caltrans engineers. There are two possible approaches:

1. build a downloadable, self-installable distribution that can automatically check for updates, similar offline version of MS Office;
2. establish online interface, by means of which spreadsheets with simulation input and data can be exchanged between the user and the server running the computational tasks.

In both cases, the software will remain open source and free. We recommend the second approach as more efficient of the two. Moreover, it will allow to connect simulation data with online maps, such as Google Maps or Bing.

Bibliography

[1] Berkeley Advanced Traffic Simulator. `http://github.com/calpath/beats`.

[2] Connected Corridors Program. `http://connected-corridors.berkeley.edu`.

[3] HOT Lane Simulation Tools — UCTC Project Data. `http://github.com/akurzhan/L0-planning/tree/master/config/UCTC2014_SimulationData`.

[4] Simulation Framework. `http://github.com/akurzhan/L0-planning`.

[5] California Department of Tranportation. PeMS homepage. `http://pems.dot.ca.gov`.

[6] Michael J. Cassidy, Kwangho Kim, Wei Ni, and Weihua Gu. A problem of limited-access special lanes. Part I: Spatiotemporal studies of real freeway traffic. *Transportation Research Part A: Policy and Practice*, In press, 2015.

[7] R. Courant, K. Friedrichs, and H. Lewy. Über die partiellen Differenzengleichungen der mathematischen Physik. *Mathematische Annalen*, 100(1):32–74, 1928.

[8] G. Dervisoglu, G. Gomes, J. Kwon, A. Muralidharan, P. Varaiya, and R. Horowitz. Automatic calibration of the fundamental diagram and empirical obsevations on capacity. *88th Annual Meeting of the Transportation Research Board, Washington, D.C., USA*, 2009.

[9] K. Jang and M. Cassidy. Dual influences on vehicle speed in special-use lanes and critique of US regulation. *Transportation Research, Part A*, 46(2012):1108–1123, 2012.

[10] A. A. Kurzhanskiy and P. Varaiya. Active traffic management on road networks: a macroscopic approach. *Phil. Trans. R. Soc. A*, 368:4607–4626, 2010.

[11] A. A. Kurzhanskiy and P. Varaiya. Traffic management: An outlook. *Economics of Transportation*, 4(3):135–146, 2015.

[12] Los Angeles County Metropolitan Transportation Authority. Metro Express Lanes. `http://www.metroexpresslanes.net`.

[13] Metropolitan Transportation Commission. Bay Area Express Lanes. `http://bayareaexpresslanes.org`.

[14] Inc. System Metrics Group. Contra Costa County I-680 Corridor System Management Plan Final Report. Technical report, Caltrans District 4, 2015. `http://dot.ca.gov/hq/tpp/corridor-mobility/CSMPs/d4_CSMPs/D04_I680_CSMP_Final_Revised_Report_2015-05-29.pdf`.

[15] C. M. J. Tampère, R. Corthout, D. Cattrysse, and L. H. Immers. A generic class of first order node models for dynamic macroscopic simulation of traffic flows. *Transportation Research, Part B*, 45(1):289–309, 2011.

[16] TOPL. TOPL homepage, 2006-2011. `http://ucb-trans.org/topl/`.

[17] M. Wright, G. Gomes, R. Horowitz, and A. A. Kurzhanskiy. On node and route choice models for high-dimensional road networks. 2016. `http://arxiv.org/abs/1601.01054`.